AD NUMBER

**AD867872**

LIMITATION CHANGES

TO:

**Approved for public release; distribution is unlimited. Document partially illegible.**

FROM:

**Distribution authorized to DoD only; Administrative/Operational Use; DEC 1969. Other requests shall be referred to Army Electronics Command, Attn: AMSEL-HL-CT-P, Fort Monmouth, NJ 07703. Document partially illegible.**

AUTHORITY

**USAEC ltr, 23 Aug 1973**

AD

TECHNICAL REPORT ECOM-0378-4

# SIGNAL PROCESSING TECHNIQUES FOR SOUND RANGING: FROM CORRELATION FUNCTIONS TO TARGET COORDINATES

INTERIM REPORT





DECEMBER 1969

ECOM

UNITED STATES ARMY ELECTRONICS COMMAND · FORT MONMOUTH, N.J.

CONTRACT DAAB07-67-C-0378

BOLT BERANEK & NEWMAN INC.
50 Moulton St. Cambridge, Mass.

# DISCLAIMER NOTICE

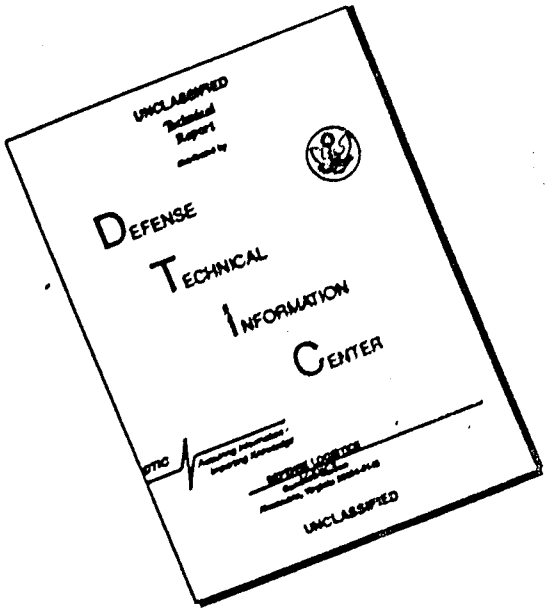


THIS DOCUMENT IS BEST QUALITY AVAILABLE. THE COPY FURNISHED TO DTIC CONTAINED A SIGNIFICANT NUMBER OF PAGES WHICH DO NOT REPRODUCE LEGIBLY.

# NOTICES

## Disclaimers

The findings in this report are not to be construed as an official Department of the Army position, unless so designated by other authorized documents.

The citation of trade names and names of manufacturers in this report is not to be construed as official Government indorsement or approval of commercial products or services referenced herein.

## Disposition

Destroy this report when it is no longer needed. Do not return it to the originator.

TR ECOM-0378-4

Reports Control Symbol OSD-1366
December 1969

# SIGNAL PROCESSING TECHNIQUES FOR SOUND RANGING: FROM CORRELATION FUNCTIONS TO TARGET COORDINATES

Interim Report
1 January 1968 – 31 October 1968

Contract No. DAAB07-67-C-0378
DA Project No. 1Z6 62704 D198 02

prepared by

BOLT BERANEK AND NEWMAN INC.
Cambridge, Massachusetts

for

U.S. ARMY ELECTRONICS COMMAND
Fort Monmouth, New Jersey

## SUMMARY

This report considers the problem of predicting target coordinates, given a temporal and spatial distribution of shots from a multiplicity of targets. Our method is based on analyzing multifold polarity-coincidence correlations of acoustic signals received at a configuration of azimuth-determining arrays.

We review the process of generating multifold correlation functions, with emphasis on those properties which are of concern in azimuth determination. We describe an azimuth determination algorithm designed to make most effective use of the information contained in the correlation function.

Our discussion of generalized triangulation points out the weaknesses of traditional methods, and outlines a probabilistic approach to triangulation that would yield an optimal prediction for a given set of azimuths. Because this probabilistic approach would be extremely demanding in computational requirements, we present an alternative method based on similar concepts but yielding a closed-form solution. This new method of generalized triangulation is tested with synthetic data, and found consistently more accurate than the traditional method.

# FOREWORD

This report documents progress in research and development of a signal processing technique for sound ranging. Some of the technical discussion requires a general knowledge of previous reports; but the reader unfamiliar with those reports should still find the problems discussed here both coherent and generally interesting.

Overall, this investigation aims at designing a data-processing system that will perform most accurately and rapidly the signal analysis required by the BBN sound-ranging system. In the previously reported work, we described a system capable of yielding correlograms automatically in virtually real time. These correlograms represent, as a function of the azimuthal angle, the values of a fourfold correlation of acoustic signals received at the microphones of an array. The laboratory sound-ranging system generates a correlogram approximately every half second, with a resolution of one-half degree of azimuthal angle. In the absence of noise, maxima in the correlograms should occur at angles which correspond, within ± 1/4°, to the azimuths from which sounds are received. In the current report, we begin by assuming many correlation functions. Our problem is to obtain valid target coordinates from such a sequence of correlograms.

TABLE OF CONTENTS

page

## LIST OF FIGURES

## LIST OF TABLES

# TECHNICAL DISCUSSION

## 1.0 INTRODUCTION

The process of sound ranging locates a target by means of a multi-array configuration of azimuth-determining arrays. In previous reports,[1,2,3] we described how each array yields, as a function of azimuthal angle, a multifold polarity-coincidence correlation (PCC) count of the signals detected at its constituent receivers. This report examines the problem of determining weighted sets of target coordinates from the information contained in these correlation functions. The procedure to be followed consists of a series of relatively independent steps, illustrated in Fig. 1 and outlined below.

Assume that there exists in the vicinity of the sound-ranging system a number of targets, each of which produces a series of shots at unknown times. When the signal from a shot impinges on an array, it generates a peak in the correlation count obtained at that array. As a first step then, we must determine the direction of each shot relative to each array. Although one can approximate these directions simply by observing the angular position of each correlation maximum, the approximation will be distorted by ambient noise and the microphone spectral characteristics, which give rise to spurious correlation maxima, and shift and distort the true maxima. In addition, closely spaced peaks may be attributed to either the distortion of a single peak or to the arrival of a number of shot signals from almost the same direction at almost the same time. The azimuth determination algorithm should take these difficulties into account, reject all spurious azimuths, and arrive at the best approximations to the true azimuths. The result of the azimuth determination algorithm is a list, for each array, of the azimuths and associated reception times of the shot signals.

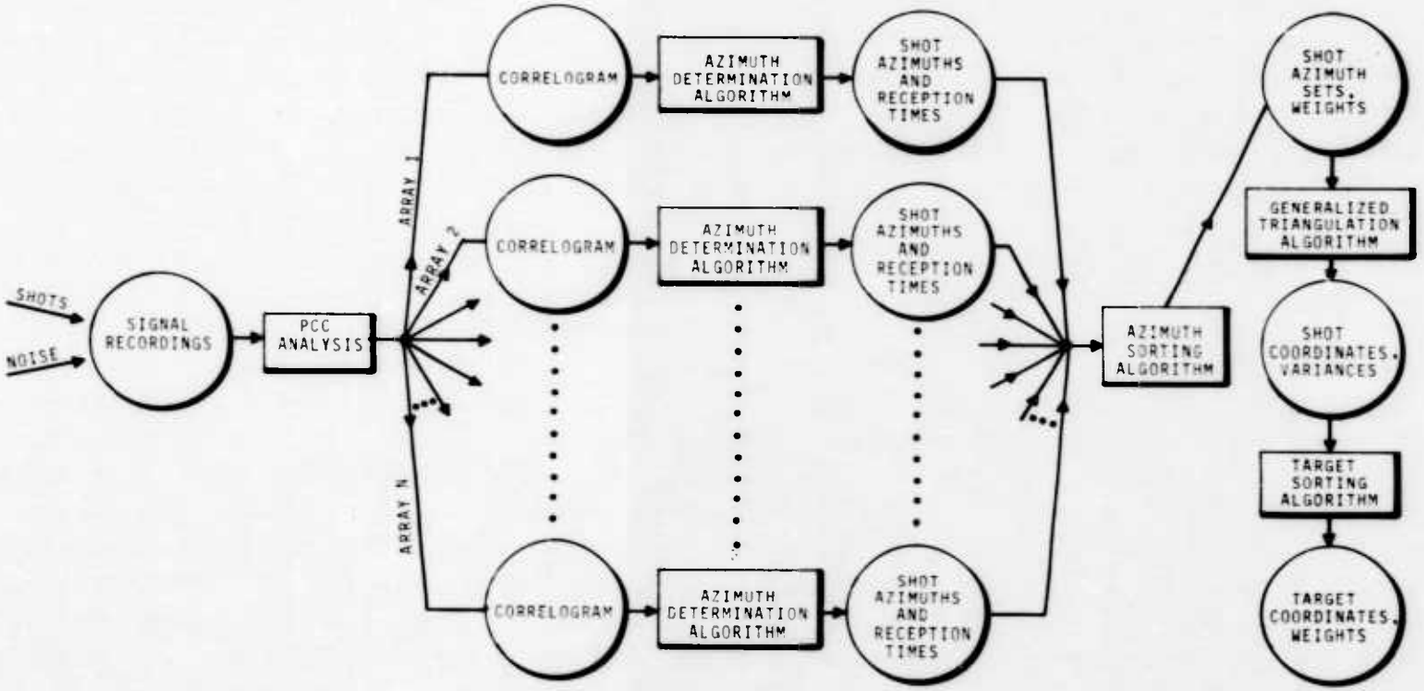


FIG.1 THE PROCESS OF GENERATING TARGET PREDICTIONS FROM SHOT SIGNALS

The second step in the procedure is to sort the azimuth lists and obtain, for each shot, a set of N azimuths, one for each of the N arrays in the configuration. If the shots are amply spaced in time and azimuth, this is a simple task. But, during rapid-fire sequences, shot signals are received at short intervals from the same general direction. Further, the individual azimuth determinations are inexact owing to the effects of noise and also to the system's intrinsic quantization of azimuthal angle (0.5°) and reception times (0.5 sec). In some cases, it may actually be impossible to establish unambiguously a unique set or sorting of azimuths for each detected shot. Through the use of heuristic programming, the system rapidly decides on a best-possible sorting of azimuths in cases where there is no unique correct sorting. The inherent uncertainties can be incorporated into a weighting factor for each set of shot azimuths.

In the ideal case, each set of shot azimuths would intersect at a single point, thus specifying uniquely the origin of each shot. In reality, the shot azimuths intersect in pairs at different locations; the derivation of a pair of shot coordinates requires a *generalized triangulation algorithm*. The specification of the shot coordinates by means of some average and variance of the shot azimuth intersection points (the usual approach to the problem) has little basis in theory and may lead to serious difficulties; for example, small errors in azimuth determination may induce extremely large (even infinite) errors in shot location. By considering the bearing lines themselves, rather than their intersection points, one can derive generalized triangulation methods – with a sounder basis in theory – that reduce these difficulties.

In the event that more than one shot emanates from each target, as a final step we must deduce target coordinates from the multitude of shot coordinates. For this purpose, the *target sorting algorithm* decides how far apart two shot locations must be in

order to be assigned to separate targets. We expect that the weights generated in the sorting procedure and the variances computed in the generalized triangulation procedure will play a principal role here, both in distinguishing the targets and in assigning final weights to them.

In the entire sound-ranging process, one must consider the influence of the array configuration itself on the accuracy of the final target locations. For a given error distribution function of the individual azimuth determinations, the target location error (as a function of range and azimuth) will depend critically on the number of arrays and on the manner in which they are deployed. If we can obtain an analytical representation of the target location error as a function of the multi-array geometry, we can then study the problem of optimizing the array deployment using logistic considerations as constraints.

In the absence of actual field data, we have resorted to the use of synthetic data for initial study of the effectiveness of the various algorithms. By assuming shot locations and times, meteorological conditions, array deployment, microphone characteristics, and source and noise spectra, we can simulate reasonably accurately the correlation functions which would be obtained from each array in the field.[1] To test only the triangulation scheme itself we simulated shot azimuths directly by postulating a particular error distribution for the azimuth determination algorithm. Although each step in the target location procedure has a sound analytical basis, we may expect that the use of such synthetic data will be of great help in arriving at the final form of the program.

In this report, we limit our discussion to the subjects of azimuth determination and generalized triangulation. We have completed the development of a satisfactory heuristic azimuth sorting algorithm, and preliminary hand analysis with synthetic data indicates that the algorithm yields excellent results in sorting shots

recorded within small spreads of time and azimuth. However, we expect that the algorithm will be subjected to a number of refinements and improvements during the course of the extensive tests of the computer programs now underway. We shall therefore postpone our presentation of the azimuth sorting algorithm to a future report.

## 2.0 AZIMUTH DETERMINATION

Before proceeding to a description of our azimuth determination algorithm, we review briefly the process by which the correlation functions are generated and the difficulties which must be overcome in order to extract azimuths from them. More detailed accounts of these matters may be found in our previous reports.

### 2.1 The Correlation Function: Its Generation and Characteristics

Each azimuth-determining array is composed of four T-23 microphones situated at the vertices and center of an equilateral triangle with sides of 80 m. (Fig. 2). The recorded sound levels are analyzed by the computer in one-second time-bytes, each byte overlapping the preceding byte by .46 seconds. For shot signal durations less than a few tenths of a second, this procedure ensures a high probability of capturing the entirety of each signal in one or another byte. Each of the four one-second signal samples is converted into an ordered time-sequence of 1000 digits: each digit is either +1, 0, or -1 depending on whether the amplitude of that one millisecond sample has an average value greater than a, between -a and +a, or less than -a, respectively. (The adjustable constant "a" is the center clipping level.) The time-sequences are analyzed with respect to azimuthal angle by making use of the azimuthal dependence of the differences in times of arrival of a signal at the four microphones. For each 0.5° increment between 0° and 180°, we have derived a set of four integers (incremental time-delay vector) which specifies the respective shifts (in milliseconds) of the four sample sequences required to simulate most closely the theoretically determined arrival time differences for that angle. The shifted sequences are compared and the PCC count is defined as the number of instances in which all four are +1 or all four are -1.

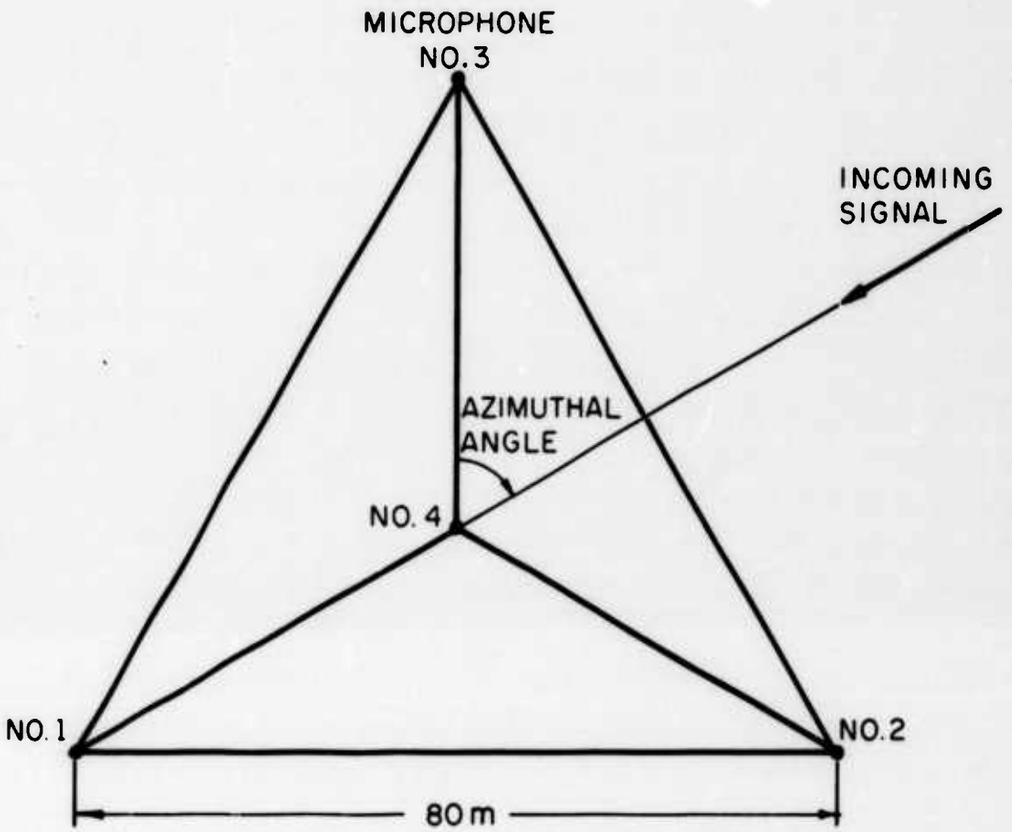


FIG. 2 THE FOUR-ELEMENT AZIMUTH-DETERMINING ARRAY

In this manner we generate a set of 360 PCC counts which may be displayed in the form of a bar graph of PCC versus azimuth. The directions of any shot signals which reach the array during the one-second time byte must be deduced from this set of 360 correlation counts.

The maximum possible PCC count is 1000. However, for typical center clipping levels and shot signal durations, the maximum counts will rarely exceed 100.

The major purpose of the center clipping is to reduce the deleterious effects of extraneous noise. In the absence of any shot signal and with no center clipping, independent random noise at each microphone generates an average PCC count of 125 at each angle since, in each millisecond, there is a 1/16 probability that all four samples are positive and a 1/16 probability that all four are negative. When a shot signal is also present, this constant "PCC background noise" makes the azimuth determination analysis more difficult. A center clipping level "a" equal to the rms noise level reduces the average PCC noise contribution by 99%.[2] Of course, the shot signal level must be appreciably larger than the noise level in order that it not be removed also; but an input signal-to-noise ratio of one to two dB appears to ensure adequate performance.

The following Figures of simulated signal recordings and their associated PCC bar graphs illustrate the important aspects of the correlation function. In Fig. 3, we reproduce the recordings which would be obtained at the four microphones of an array under the following ideal conditions: (1) a typical "N-wave" pressure pulse incident on the array at an azimuthal angle of 65°, (2) no background noise, (3) microphones having infinite spectral response, (4) no center clipping. The corresponding PCC bar graph has a single, well defined maximum at the correct azimuth and is

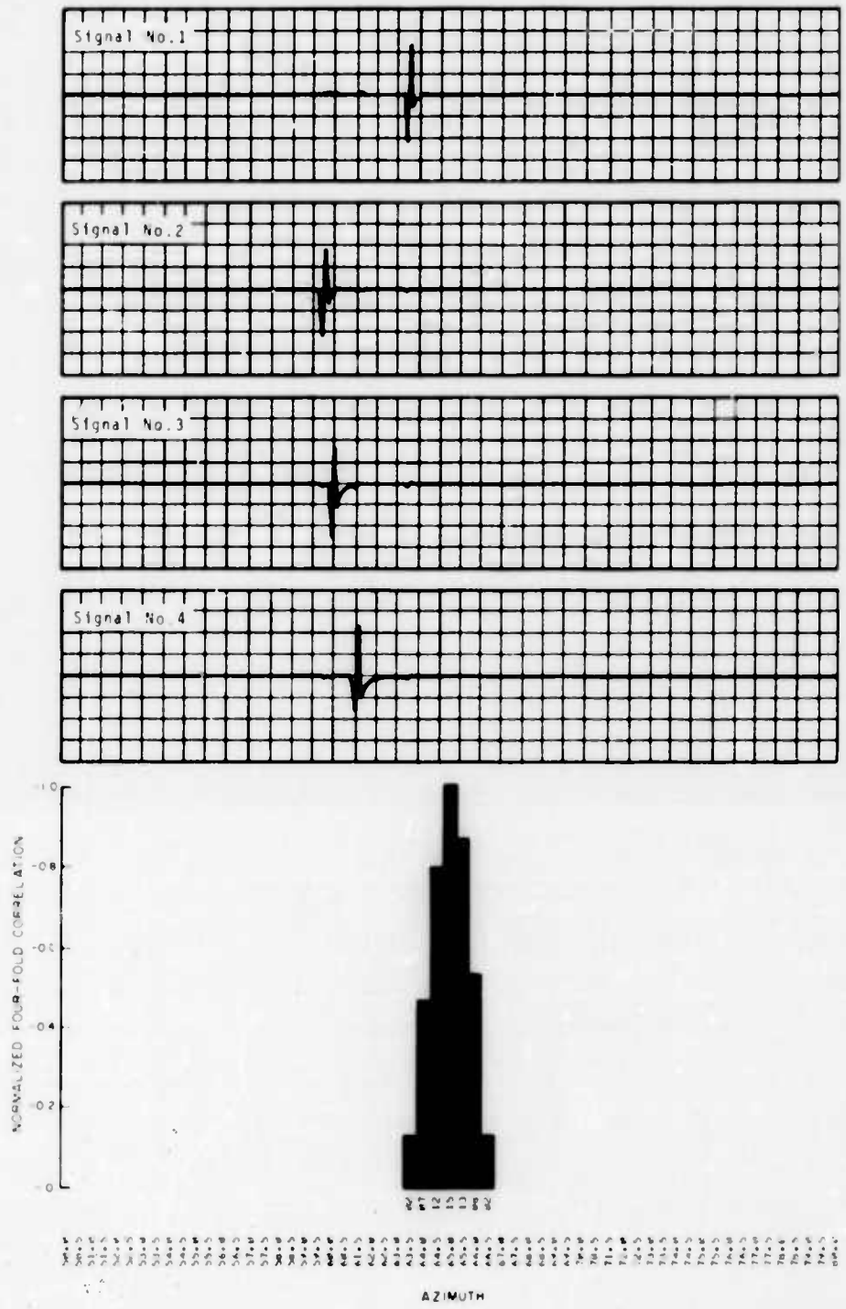


FIG.3 SIMULATED NOISELESS SIGNALS AND PCC FUNCTION: PRESSURE PULSE AT 65°

zero everywhere else. The maximum PCC count of only fifteen* is indicative of the extremely short duration of the shot signal.

Figure 4 shows the effect of having two such N-wave pressure pulses incident at the same time but at different angles (65° and 76.5°), all other conditions the same. The correlation function again has unique maxima at the correct azimuths.

Figure 5 duplicates the conditions in Fig. 3, except that we have simulated the response of actual T-23 microphones to the pulse. Acting essentially as narrowband filters, the microphones convert the pulse into a temporally extended tone burst. The principal effect on the correlation function is that the maximum PCC count is increased (from 15 to 47) as a result of the longer duration of the recorded signals.

In Fig. 6, we have the T-23 responses to the same two simultaneous pulses as in Fig. 4. Although the responses appear to be from a single shot, the correlogram shows the ability of the system to clearly separate the two signals.

In consideration of the influence of random noise on the correlation function, Fig. 7 shows the effect of superimposing independent noise on the pressure pulses of Fig. 3. In producing the correlogram, the center clipping level "a" was set so that the noise observed on the recordings, without the signal, exceeded "a" approximately 5% of the time. Comparing the correlograms of Figs. 3 and 7, we note the following consequences of the introduction of noise: (1) a random modulation of the correlation peak, which in turn distorts the angular location of the maximum PCC count, (2) small localized correlation counts at angles far removed from the signal maximum (the correlation response for angles

---

*The bar graphs in these Figures represent the PCC counts normalized to the largest count; the actual number of counts corresponding to each bar is indicated by the number at its base.

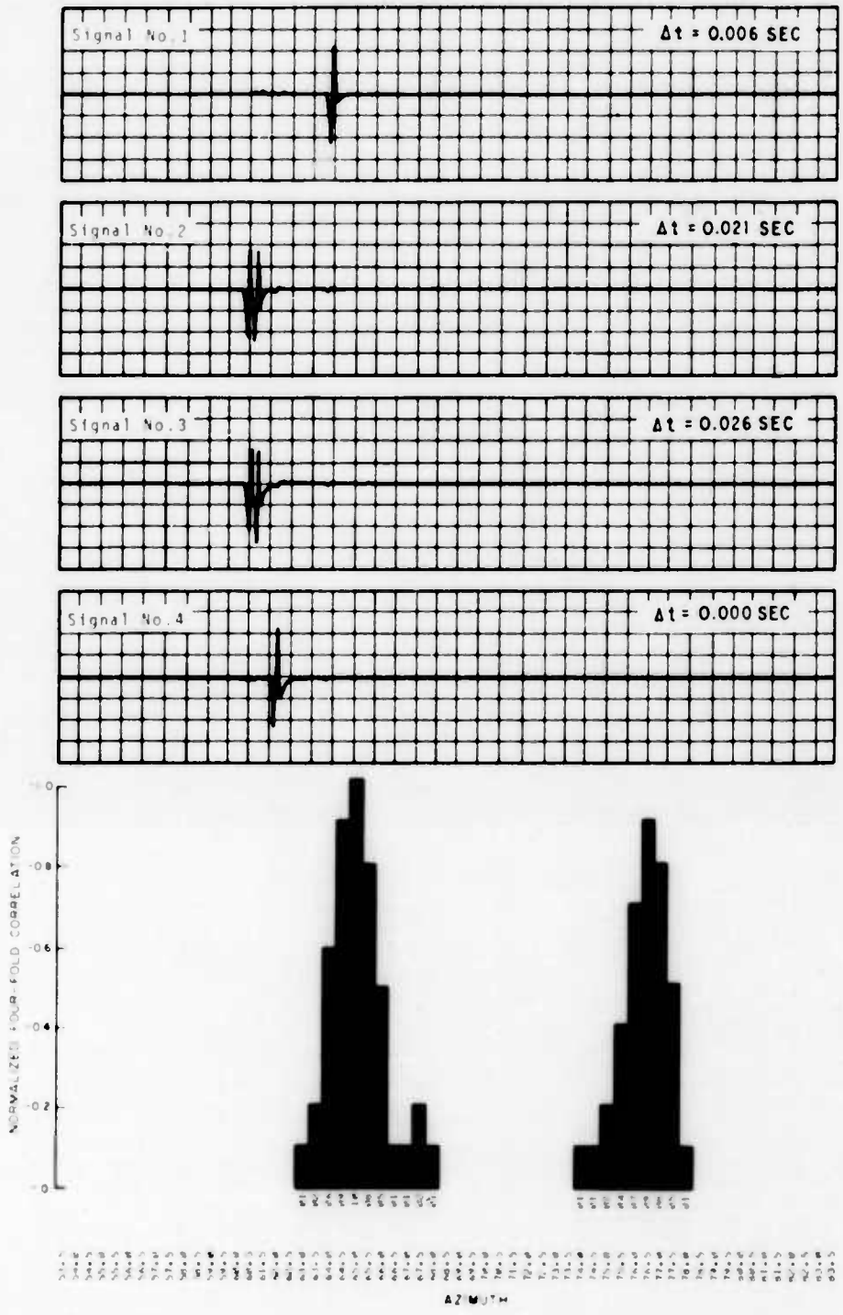


FIG.4 SIMULATED NOISELESS SIGNALS AND PCC FUNCTION: TWO SIMULTANEOUS PRESSURE PULSES AT 65° AND 76.5°

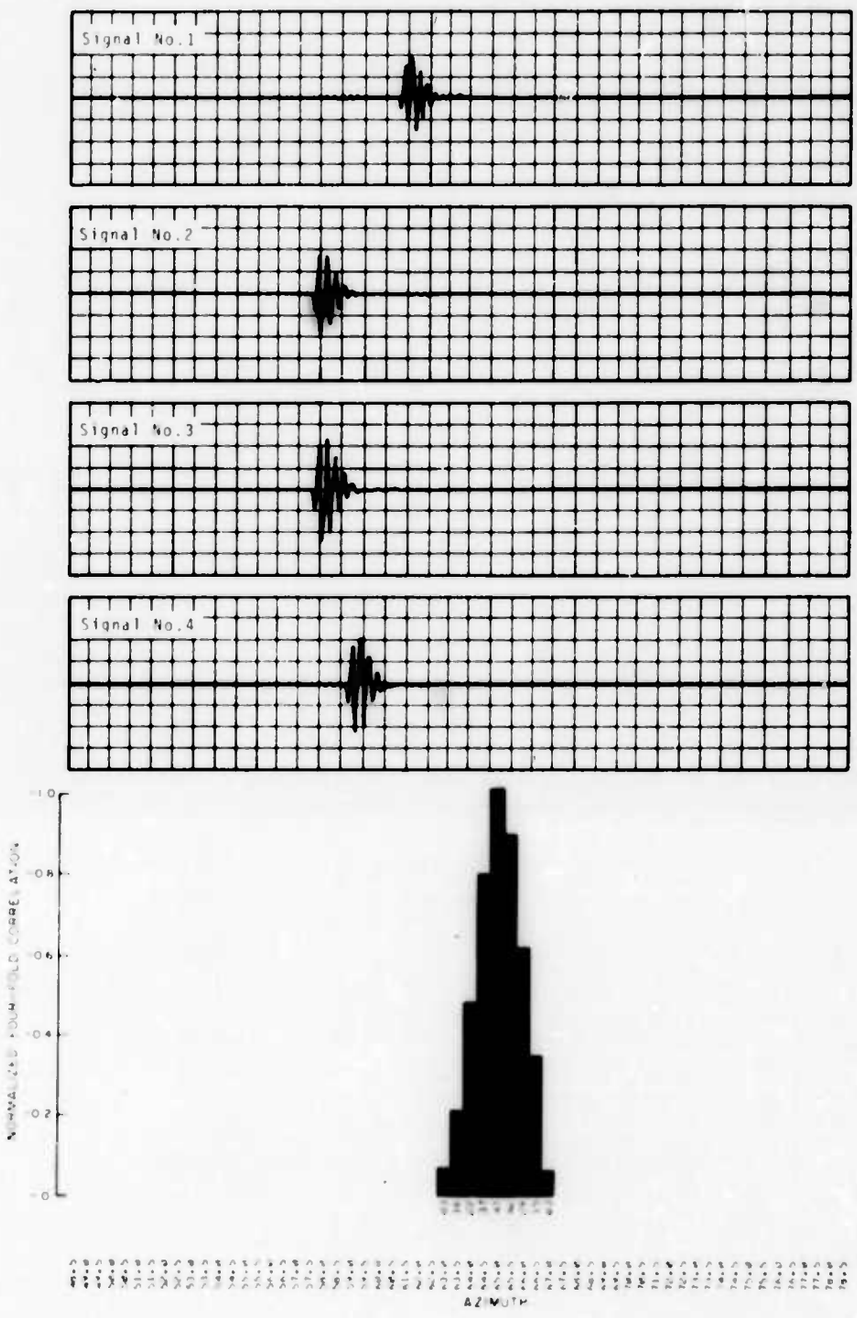


FIG.5 SIMULATED NOISELESS T-23 RESPONSES AND PCC FUNCTION: PRESSURE PULSE AT 65°

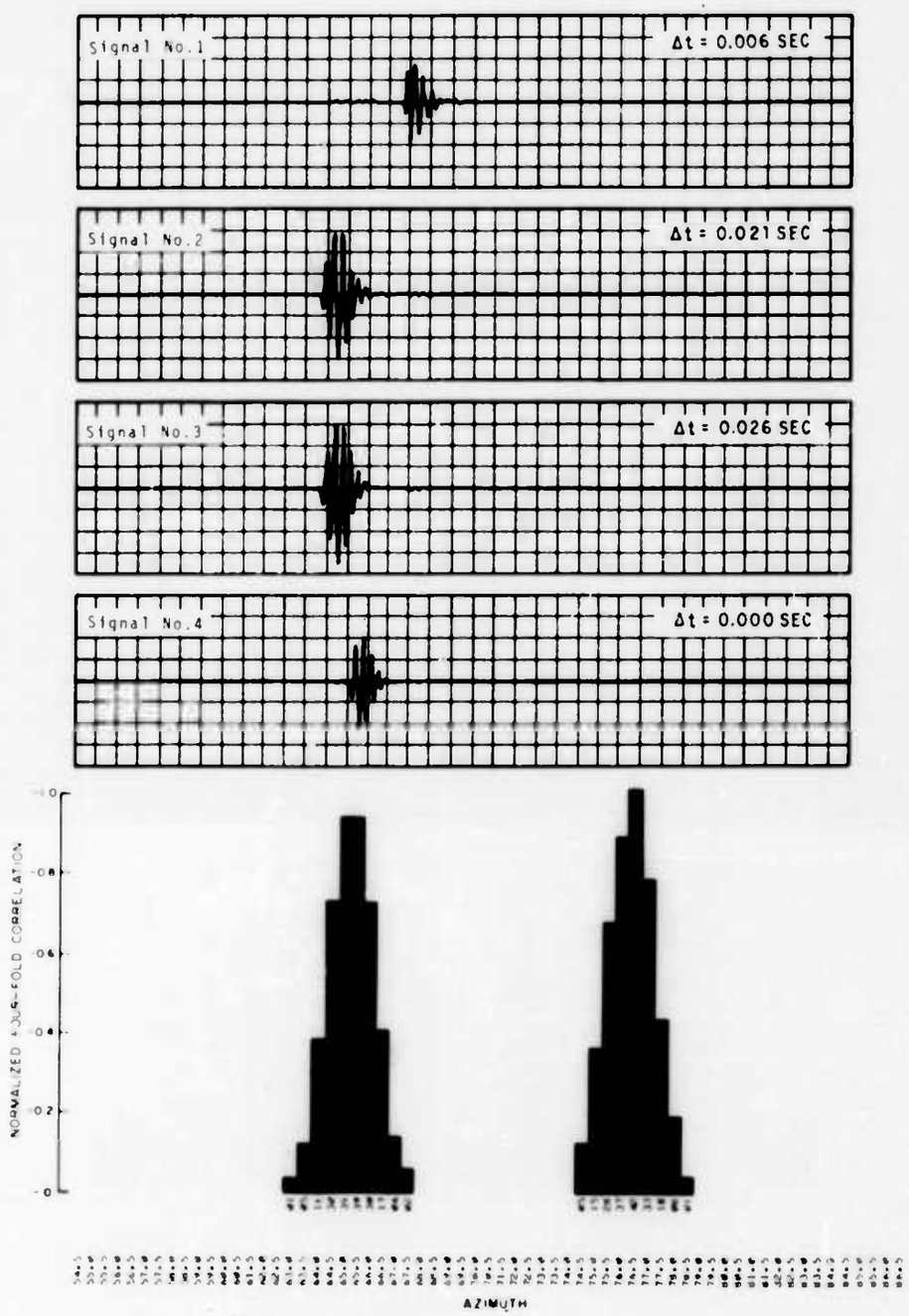


FIG.6 SIMULATED NOISELESS T-23 RESPONSES AND PCC FUNCTION: TWO SIMULTANEOUS PRESSURE PULSES AT 65° AND 76.5°

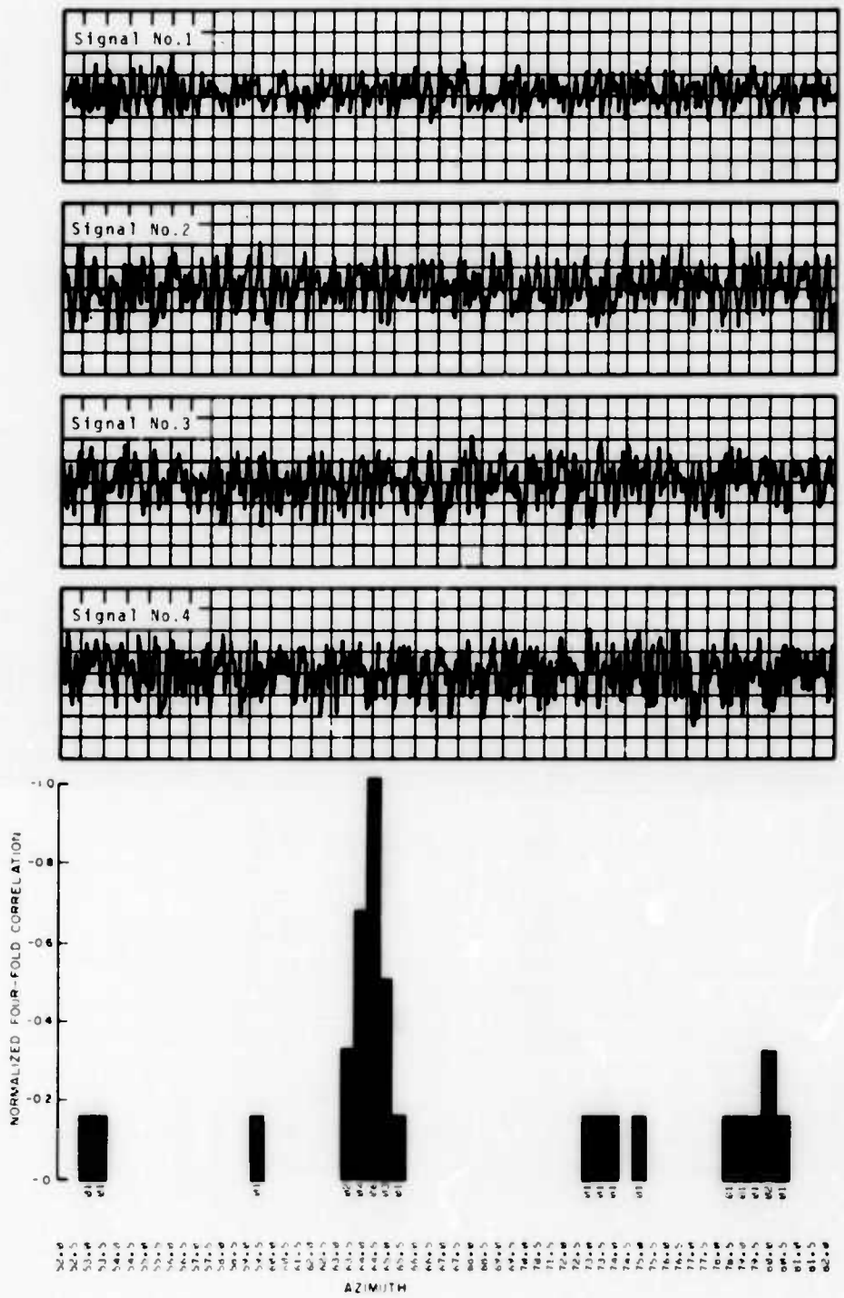


FIG.7 SIMULATED SIGNALS,WITH INDEPENDENT NOISE,AND PCC FUNCTION: PRESSURE PULSE AT 65°, INPUT THRESHOLD SENSITIVITY AT .05

outside the range illustrated was no higher than the highest noise response in the displayed portion) and, (3) the center clipping used to reduce the noise response also reduces the correlation response of the signal itself (in this case, from 15 to 6).

The preceding examples illustrate the principal difficulties which must be overcome by a satisfactory azimuth determination algorithm; it must (1) reject all secondary correlations due to noise, (2) recognize and accept all correlations due to actual shot signals, (3) decide whether overlapping correlation peaks represent distortion of a single peak or the presence of more than one shot signal and, (4) make best-possible estimates of the azimuths of all shot signals.

## 2.2 The Azimuth Determination Algorithm

The following subsections describe elements of the algorithm as implemented in our present system; we have also suggested possible improvements for a future system. The algorithm involves a number of constants whose values we have not specified. The optimal choices for these constants must await the exercising of the program with synthetic data or, where possible, with actual field data.

### 2.2.1 Correlation threshold and maximum test

This test is designed to eliminate the small local PCC counts caused by noise and to identify any present signal correlation peaks. We define the *mean correlation* M as the average of the 360 PCC counts. The *minimal signal correlation* S is defined as a linear function bM + c of the mean. If the largest count is less than S, we assume that no signal is present and the analysis is terminated. The *correlation threshold* T is defined as another

linear function dM + e of the mean, such that only a small fraction (perhaps 10%) of all the nonzero counts are greater than T. The threshold is subtracted from each count, thus removing most, and possibly all, of the noise contribution.

### 2.2.2 Group weight test

A *correlation group* is defined as a set of three or more consecutive nonzero PCC counts. All counts which do not belong to any group are eliminated. The *weight* of a group is the sum of its component counts. The *average weight* of a group is its weight divided by the number of counts it contains. Any group whose average weight is less than a predetermined *minimum weight* W is eliminated. This test should remove any vestigal noise contributions.

### 2.2.3 Group azimuths and group overlap test

Starting at the beginning of each group, we add the counts in the group until the sum most nearly equals half the group weight. The azimuth of the last count in the sum is the *group azimuth*. Thus, the azimuth associated with each group is the azimuth which bisects the "area" of the group (which is not necessarily the azimuth having the largest PCC count in the group). The most probable position of this half-area azimuth is the position of the original (noiseless) peak, since the random noise adds, on the average, as many counts to one side of the original peak as to the other. Thus, the above procedure should provide an effective means of allowing for noise-induced distortion of the correlation peaks.

If either (a) the PCC count at the group azimuth is the maximum count in the group, or (b) the maximum count in the group exceeds the group-azimuth count by less than a predetermined *overlap test constant* G, then the original group azimuth is retained.

However, if the maximum count in the group exceeds the group-azimuth count by more than G, we subtract the group-azimuth count from each count in the group and repeat the analysis (i.e., find group azimuth, do overlap test) for each of the new groups thus generated. In Fig. 8, we illustrate the overlap test with a typical example of overlapping correlation groups.

We may expect that this analysis will fail if two signal groups overlap to such an extent that their "sideskirts" sum to a larger count than either of their maxima. It would then be extremely difficult to detect the presence of two separate shot signals. This problem might be circumvented under certain conditions by making use of the shot azimuths determined at the other arrays of the configuration during the same time byte. If the two signal groups at the other arrays have sufficient angular separation to be resolved, it would then be clear that there was a "missing" azimuth at one array; the single azimuth found at that array would be counted twice in the azimuth sorting process.

### 2.2.4 Use of overlapping azimuth intervals

In the algorithm described above, we analyze all counts in the entire 180° azimuth span at once; but we can reduce the computer storage requirements by dividing the correlation function into a number of azimuthal segments and exercising the algorithm on each segment separately. To ensure that individual groups are not split up, the segments should overlap by an amount that is large in comparison to the maximum expected azimuthal spread of a signal group. We currently use five 50° segments with 17.5° overlaps.

① SPECIFY OVERLAP TEST CONSTANT: G = 3

② EXHIBIT THE GROUP:

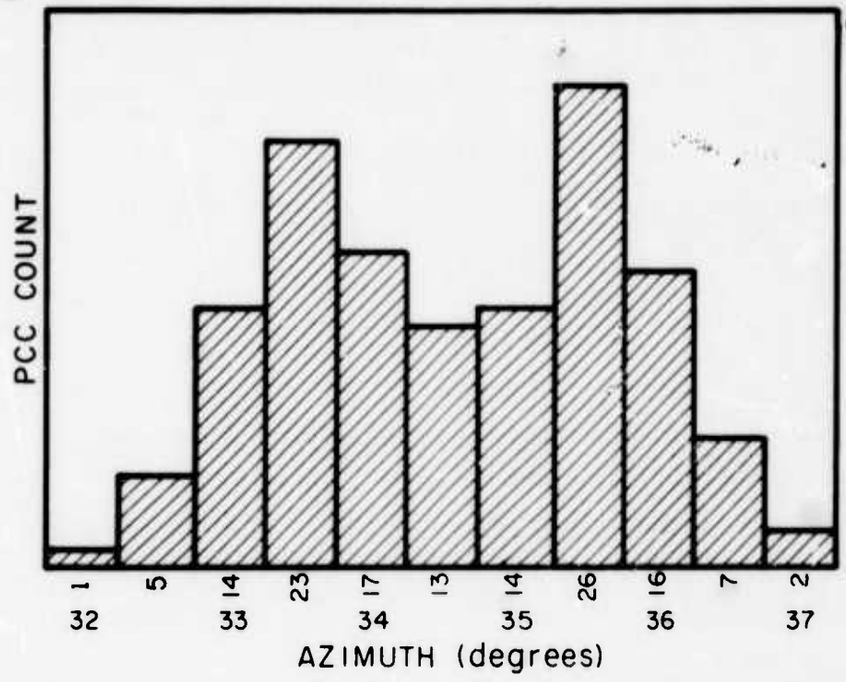


③ CALCULATE:

Group weight=138
Group azimuth=34.5°

④ PERFORM OVERLAP TEST: (Max. count - group azimuth count)=(26-13)>G

⑤ SUBTRACT GROUP-AZIMUTH COUNT, EXHIBIT NEW GROUPS:

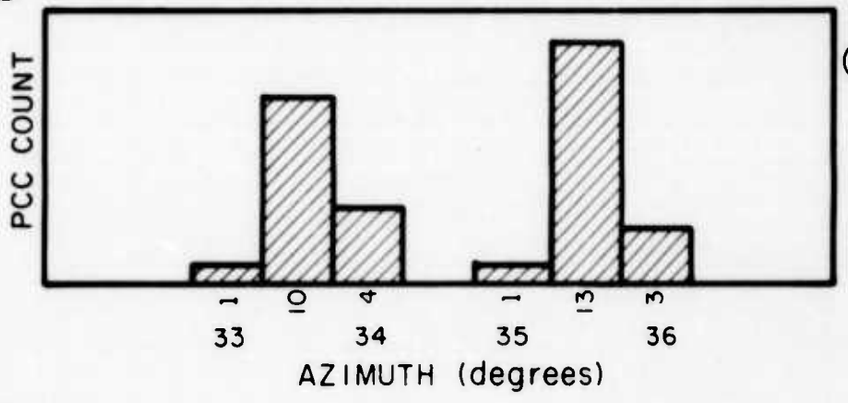


⑥ CALCULATE:

Group weights=15,17
Group azimuths=33.5°
35.5°

⑦ PERFORM OVERLAP TEST: (Max. count - group azimuth count) = $\begin{cases}(10-10)=0\\(13-13)=0\end{cases}$

⑧ FINAL GROUP AZIMUTHS: 33.5°, 35.5°

FIG.8 AN EXAMPLE OF THE GROUP OVERLAP TEST

## 3.0 GENERALIZED TRIANGULATION

When we have a set of shot azimuths generated by several shots at different targets and no *a priori* knowledge of the correspondence of shots and azimuths, we must first select subsets of shot azimuths corresponding to individual shots. By azimuth sorting, we obtain sets of N shot azimuths (assuming an N-array configuration), each set corresponding to a unique shot. We must then consider the most appropriate generalized triangulation procedure for deducing a shot location given a set of N intersecting bearing lines.

Traditional sorting methods tend to rely to some degree on finding azimuths whose pairwise intersection points are grouped in small clusters. Such sorting methods involve implicit assumptions that the subsequent generalized triangulation procedure should be based primarily on the positions of the intercepts, and that the closeness of intercepts is a valid criterion for the reliability of a target prediction. In this Section, we shall show that these assumptions do not necessarily lead to realistic target locations. Instead, a proper generalized triangulation scheme should emphasize the relationship of the shot prediction to the bearing lines themselves, rather than to their intersection points. In a future report, we will explore this concept in connection with the sorting procedure.

### 3.1 Generalized Triangulation Using Azimuth Intersections

Consider first the simplest case of just two intersecting bearing lines. The point of intersection is then the only reasonable shot location prediction. The displacement of this prediction from the true shot location depends on the accuracy of the bearings and on the angle at which they intersect. Suppose that the bearings intersect at a small angle $\phi$, that the uncertainty of

each bearing is an angle $\Delta\phi$, that the range from the center of the array configuration to the intersection point is R, and that R is much greater than the interarray spacing. Then there is an uncertainty of approximately $2R\Delta\phi/\phi$ in the range to the shot, and an uncertainty of approximately $R\Delta\phi$ in a direction perpendicular to the direction of the range. For shot locations whose bearings subtend small angles with respect to the line joining the two arrays, the range uncertainty is a large fraction of the range itself.

We might intuitively expect that, if we obtain a third bearing, the triangle determined by the addition of the third bearing would have a high probability of enclosing the true shot location. To understand why this is not in fact the case, let us assume that the bearing errors are distributed symmetrically; i.e., the true shot location is equally likely to be on either side of any bearing line. It follows then that the probability of the shot being in any one of the four sectors created by the intersection of two bearing lines is one-fourth. A third bearing line could determine a triangle by closing off either of two opposing sectors. The triangle formed by closing off either sector would have a 1/8 probability of enclosing the shot. The total probability that the shot is within the triangle is therefore one-fourth. With only 25% confidence that the shot is in the triangle, we conclude that the triangle generated by the intersections of three bearing lines is a questionable improvement over the single point generated by the intersection of two bearing lines.

When an even larger number of bearings are available, the intersection points may be distributed over a large area and will not usually define a single closed polygon. An intuitive approach might lead us to specify the shot location by means of some average of all the intersection points. In the next subsection, we describe an algorithm based on this approach and show some of the difficulties associated with it.

### 3.1.1 Method of the mean of the intersections (MI)

A set of N shot azimuths in general defines N(N-1)/2 intersection points; the number of intersections is smaller if some of the azimuths are parallel. Given the position of each azimuth-determining array, the x and y coordinates of the intersection points relative to some fixed origin can be calculated by means of standard trigonometric formulas. The shot location coordinates are obtained by averaging separately the x and y coordinates of all the intersection points. We henceforth refer to this algorithm as the MI method.

### 3.1.2 Inadequacies of the MI method

The most obvious fault of the MI method is that it fails completely if any azimuths are parallel: the predicted shot location is then at infinity.

Another drawback is that the prediction may be very sensitive to small errors in the individual azimuth determinations. Consider, for example, the intersections of the four bearing lines shown in Fig. 9. The solid lines create six intersections whose mean is shown by the dot enclosed by a solid circle. The dashed lines represent an alternative set of bearing lines chosen at random under the condition that their directions differ from the original directions by no more than a small assumed angular uncertainty. The alternate bearing lines form intersections that shift the prediction to the point indicated by the dot enclosed by a dashed circle. Assume that the original prediction is close to the true shot location. Although two of the alternate bearing lines pass closer to the shot than the corresponding solid lines, the alternate prediction is nonetheless poorer than the original prediction.

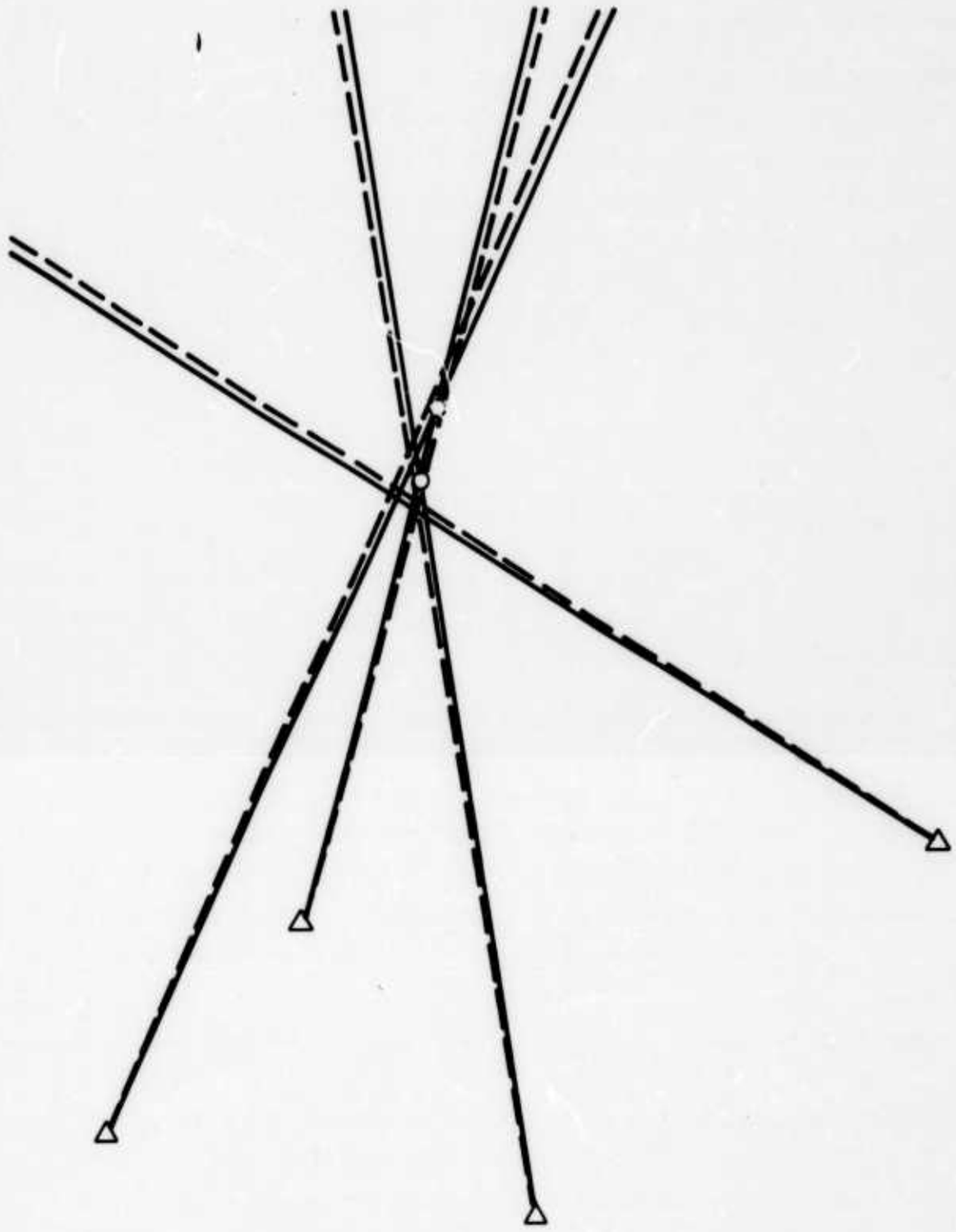

FIG.9 SENSITIVITY OF AN MI PREDICTION TO AZIMUTH UNCERTAINTIES

A common method of reducing these difficulties is simply to discard (or assign small weight to) intersections which are far removed from the mean. This is a rather artificial procedure and, moreover, it offers no guarantee that the prediction obtained from the surviving azimuths will be better than the original prediction. Furthermore, if we have only three bearing lines, there is no obvious criterion for determining which intersection is the "bad" one.

## 3.2 The Probabilistic Approach

The preceding discussion leads to the conclusion that the MI triangulation method is not based on sound analytical concepts. Indeed, thus far little fundamental research has been devoted to the problem of determining an optimal generalized triangulation algorithm. We outline below an extremely general approach to this problem, the implications of which we hope to develop more fully in our future work.

Our main point is that the prediction of a shot location is essentially a statistical process. We are presented with a set of bearing lines and associated statistical uncertainties; our goal should be to determine that point on the plane which has the greatest probability of coinciding with the shot location. To accomplish this, we may transform the probability functions of the individual azimuth uncertainties into a probability function for points on the plane. The resulting two-dimensional probability function would contain a large amount of useful information. Its maximum would, of course, determine the best shot location prediction. The height at the maximum point, the steepness of the probability surface in the vicinity of the maximum point, and the mean level of the probability function outside the region of the maximum would be some measure of the reliability of the prediction.

A simple way to visualize the process is to imagine a set of translucent overlays, on each of which is imprinted a variable density optical image of a bearing line and its associated probability density. The image is most dense along the bearing line. The density decreases for azimuths on either side of the bearing line and approaches zero (i.e., transparency) for azimuths further from the bearing line than the assumed uncertainty of the azimuth determination. The overlays are placed on top of one another on a target map in such a way that each bearing line passes through the appropriate array position at the correct angle. The point on the map at which the combined overlays are most opaque would then be the most probable shot location.

The analytical implementation of the process requires an assumption as to the statistics of the azimuth uncertainties. We could assume a Gaussian distribution of the deviation of an azimuth from the mean, with a variance proportional to the expected uncertainty. We must then find the geometrical transformation between x,y coordinates relative to some fixed origin, and range and azimuthal deviation relative to the array. The Jacobian of this transformation is required to perform the transformation of probability densities to x,y coordinates. When this is done for each array in the configuration, the final two-dimensional probability function is calculated as the product of the individual functions.

Because this method is based on the statistics of the azimuth directions themselves, and not on the statistics of the azimuth intersection points, we would expect that the prediction obtained would be quite insensitive to small individual azimuth uncertainties.

The principal drawback of the general method is that although quite simple in concept, it would be extremely demanding in computational requirements, and thus, beyond the scope of the present

system. In the next Section, we outline an alternative method which also relies on the bearing lines themselves but is more feasible in practice.

### 3.3 Generalized Triangulation Using Azimuth Displacements

In lieu of the rigorous probabilistic approach described above, we seek a generalized triangulation procedure which satisfies the following criteria:

1. The procedure should be based on some relation involving the bearing lines themselves, rather than their intersection points.
2. The shot prediction should be relatively insensitive to small deviations of the bearing line directions.
3. The method should be reasonable in computational requirements; preferably, the coordinates of the shot prediction should be expressible as a closed analytical formula, rather than as the result of a search procedure.

A method which seems to satisfy all of these criteria is based on the perpendicular distances from an assumed shot location to all of the bearing lines.

#### 3.3.1 Method of the minimum mean-square displacement (MD)

The MD prediction is defined as that point which minimizes the mean-square perpendicular distance to all bearing lines. In Appendix A, we derive simple closed formulas expressing the coordinates of the MD prediction in terms of the coordinates of the N arrays and the azimuths of the N bearing lines.

The actual value of the root-mean-square displacement of the prediction from the bearings might be a suitable measure of the

uncertainty to be assigned to the prediction. However, other measures of uncertainty should also be considered. A valid uncertainty measure should be well correlated with the actual distance from the prediction to the true shot location.

In the following subsection, we compare the relative sensitivities of the MI and MD methods to small deviations of the bearing line directions.

### 3.4 Qualitative Comparison of MD and MI Predictions

We may illustrate the major advantages of the MD method by means of some simple qualitative examples. First, we consider a linear deployment of three arrays with an interarray separation D, and a shot originating on the central axis of the configuration at a distance ΞD (Fig. 10). With a perfect azimuth determination routine, the three bearing lines would intersect at the shot location and either the MI or MD method would yield a perfect prediction (Fig. 10a). We now assume progressively larger errors in the bearing line associated with the leftmost array so that it gradually becomes parallel to the center bearing line. Figure 10b shows that if the perturbation is small, the predictions of the two methods almost coincide. As the enclosed triangle becomes more elongated, as in Fig. 10c, the MI prediction moves out from the true shot location much more rapidly than does the MD prediction. When the bearing lines become parallel, as in Fig. 10d, the MI prediction moves out to infinity, while the MD method still produces a finite prediction (although at considerable distance from the shot, displaced by approximately a 50% increase in range).

We can construct another example for which the MI method fails completely while the MD method actually yields a perfect prediction. We consider a linear four-array configuration with the shot again on the central axis (Fig. 11) and study the effect

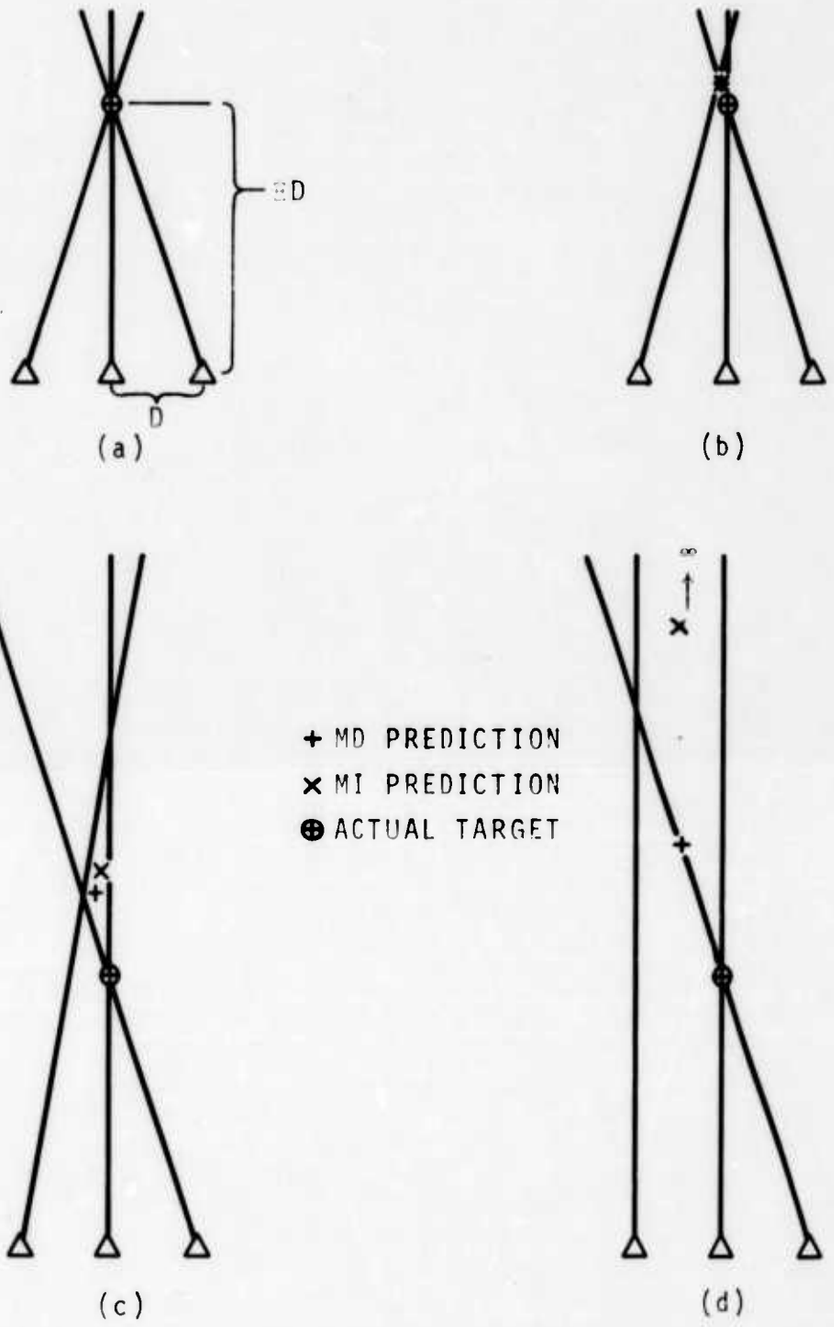


FIG.10 EXAMPLE OF PREDICTION SHIFTS FOR PERTURBATIONS OF ONE BEARING LINE OUT OF THREE

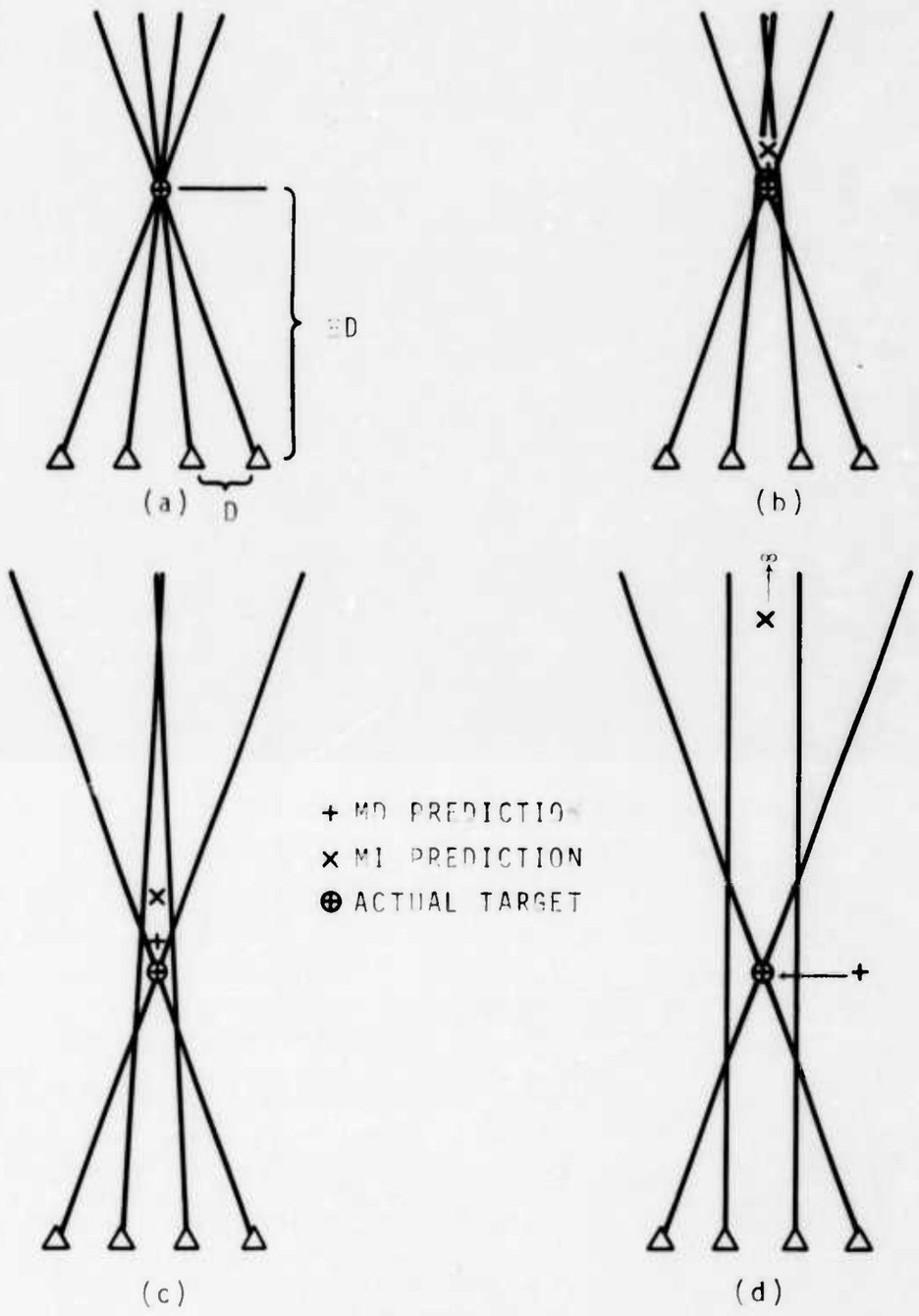


FIG. 11 EXAMPLE OF PREDICTION SHIFTS FOR PERTURBATION OF TWO BEARING LINES OUT OF FOUR

of errors which tend to make the two inner bearing lines parallel. The MI prediction again rapidly diverges as the bearing lines approach parallelism. The MD prediction moves only a small maximum distance from the shot location and then moves back to coincidence with the shot location in the limiting case. The example admittedly has an extremely unlikely symmetry; nevertheless, it dramatically illustrates the general tendency of the MD method to retain a reasonable prediction even when the MI method fails.

These examples illustrate the following important general result: an MD prediction exists as long as at least two bearing lines are not parallel. This conclusion also follows directly from the analytical formulas in Appendix A. In contrast, the MI method yields a prediction at infinity with the presence of any parallel bearing lines.

Another property of the MD method is that two parallel bearings may be replaced by a single bearing originating at a virtual array located midway between their respective arrays — and the prediction will remain unaltered. For example, in Fig. 10d the prediction is at the intersection of the bearing from the rightmost array and a bearing, parallel to the two parallel bearings, emanating from a virtual array midway between the leftmost array and the center array. Figure 11d can be described in a similar manner.

### 3.5 Quantitative Comparison of MD and MI Predictions

The generation of the synthetic data used to test our generalized triangulation algorithm is described in Appendix B. We assumed a four-array configuration consisting of arrays at the vertices and center of an equilateral triangle of side 875 m. (Fig. B-1). We postulated a set of 19 targets at various ranges and azimuths from the center of the configuration (Fig. B-2).

The ranges vary between 1.5 and 4.0 km. We further postulated that a total of 37 shots originate at the targets at specified times (Table B-I). We calculated the precise azimuth of each shot relative to the center of each array (Table B-II) and then polluted the data to simulate the azimuthal errors to be expected in a real system (Table B-III). We also computed the arrival times (rounded off to 0.5 sec) of each shot at each array.

In this subsection, we study the results of applying both the MI and MD methods to each of the 37 sets of shot azimuths in Table B-III. (We realize that in doing this, we are temporarily ignoring the azimuth sorting problem; we know that each of the 37 shot azimuths sets correponds to a unique shot because of the way in which they were generated.)

The results of the calculations are presented in Table I. For each shot, we give the difference in range and azimuth (relative to the center of the configuration) between the actual and predicted shot locations. We also give the radial error, which is the total distance of the prediction from the true shot location. In Fig. 12, we plot scale maps of the vicinity of target 1, showing the converging shot azimuths and the locations of the MI and MD predictions for shots 4, 8, and 30. Target 1 is at a range of 5000 m., so that the position of the center of the array configuration would be 11 in. to the left of the target on these maps. The array configuration would be about 2 in. on a side.

The error quantity of greatest interest in sound ranging is the normalized radial error, defined as the ratio of the radial error to the actual range of the shot. From the data of Table I, we calculated an average normalized radial error of 3.9% for the 37 MD predictions. In considering the MI predictions, we are faced with the difficulty that two predictions are infinite due to the existence of parallel bearing lines. Ignoring these two failures and averaging the other 35 MI predictions, we obtained an

TABLE I. Comparison of MD and MI shot location predictions.

| Shot | Range (km) | Radial Error | | Range Error | | Azimuthal Error | |
|---|---|---|---|---|---|---|---|
| | | MD (m) | MI (m) | MD (m) | MI (m) | MD (deg) | MI (deg) |
| 1 | 1.5 | 6 | 131 | -7 | 131 | 0.0 | -.2 |
| 2 | 1.5 | 18 | 15 | 17 | -6 | .2 | .5 |
| 3 | 1.5 | 14 | 32 | 1 | -30 | -.5 | -.4 |
| 4 | 5.0 | 311 | 462 | 310 | 462 | .3 | .1 |
| 5 | 4.0 | 152 | 1113 | -152 | -1110 | 0.0 | -1.3 |
| 6 | 4.0 | 235 | 225 | -235 | -223 | 0.0 | -.4 |
| 7 | 4.0 | 122 | 545 | -121 | -545 | 0.0 | .1 |
| 8 | 5.0 | 390 | 608 | -390 | -608 | .3 | .1 |
| 9 | 4.0 | 160 | 572 | -160 | -572 | 0.0 | -.4 |
| 10 | 3.0 | 145 | INFINITE | -145 | INFINITE | 0.0 | .5 |
| 11 | 3.0 | 154 | 305 | -154 | -305 | 0.0 | -.1 |
| 12 | 3.0 | 46 | 183 | -42 | -182 | -.3 | -.3 |
| 13 | 3.0 | 64 | 109 | 63 | -108 | 0.0 | .3 |
| 14 | 3.0 | 144 | 74 | -144 | -74 | .3 | -.2 |
| 15 | 3.0 | 155 | 86 | 154 | 86 | 0.0 | -.1 |
| 16 | 3.3 | 219 | 339 | -219 | -339 | 0.0 | .1 |
| 17 | 3.4 | 3 | 37 | 2 | -36 | .1 | .2 |
| 18 | 3.5 | 311 | 558 | 311 | 558 | .1 | -.2 |
| 19 | 3.6 | 75 | 120 | 73 | -120 | -.3 | -.0 |
| 20 | 3.7 | 207 | 1409 | 204 | 1408 | .3 | -.6 |
| 21 | 5.0 | 142 | 107 | 136 | -99 | .3 | .5 |
| 22 | 4.0 | 160 | 572 | -160 | -572 | 0.0 | -.4 |
| 23 | 4.0 | 78 | 424 | -79 | 424 | 0.0 | -.2 |
| 24 | 4.0 | 122 | 545 | -121 | -545 | 0.0 | .1 |
| 25 | 2.0 | 14 | 164 | 13 | 164 | -.3 | -.1 |
| 26 | 4.0 | 152 | 555 | -153 | -555 | 0.0 | -.3 |
| 27 | 5.0 | 506 | 48 | 505 | -24 | -.2 | -.5 |
| 28 | 4.0 | 76 | 39 | -67 | 5 | .5 | .6 |
| 29 | 4.0 | 76 | INFINITE | -75 | INFINITE | -.5 | 3.5 |
| 30 | 5.0 | 88 | 245 | 84 | 245 | .3 | .1 |
| 31 | 5.0 | 224 | 235 | 222 | -235 | .3 | -.0 |
| 32 | 4.0 | 152 | 1113 | -152 | -1110 | 0.0 | -1.3 |
| 33 | 4.0 | 334 | 216 | 334 | -215 | 0.0 | -.2 |
| 34 | 4.0 | 186 | 273 | -186 | 273 | 0.0 | -.2 |
| 35 | 2.0 | 61 | 112 | -61 | 112 | .2 | .0 |
| 36 | 4.0 | 262 | 66 | 261 | 64 | 0.0 | .2 |
| 37 | 2.0 | 15 | 28 | -1 | -23 | -.3 | -.5 |

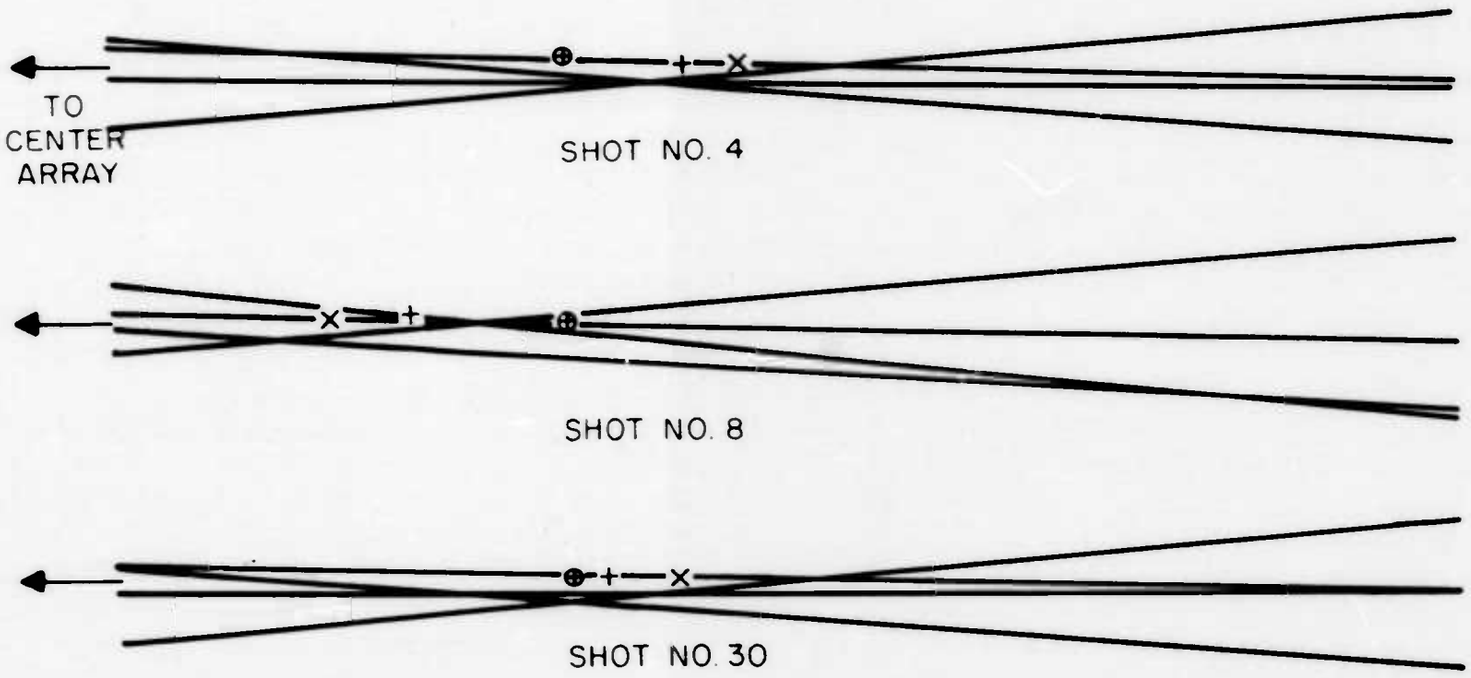


FIG. 12 MAPS OF SHOT AZIMUTHS AND PREDICTIONS IN THE VICINITY OF THE TRUE SHOT LOCATIONS

average normalized radial error of 8.9% for the MI method. In summary, we find an average radial error of about 40 m. per km. for the MD method and more than 90 m. per km. for the MI method.

The MD prediction is superior to the MI prediction in fully 28 of the 37 cases.

We are currently carrying out a similar analysis using synthetic data generated with an assumed set of targets having ranges of up to several dozen kilometers. We expect that the results will not differ markedly from those obtained here.

## 4.0 RECOMMENDATIONS

We have outlined the general procedure for predicting target locations by means of multifold correlations of received acoustic signals. We have considered in detail the steps in the procedure concerned with azimuth determination and generalized triangulation. The sorting problem will be considered in a future report.

In regard to azimuth determination, we recommend that further refinements of our algorithm be examined when the results of field tests are available. In particular, such field data should enable us to determine the optimal values of the various test constants involved in the algorithm.

In regard to generalized triangulation, we recommend that the method of minimum mean-square displacement (MD) be used in future studies. In addition, the more rigorous probabilistic approach should be studied further in order to determine whether it might be implemented in a practical system.

## APPENDIX A

### Derivation of Formulas for the MD Method of Generalized Triangulation

We wish to find expressions for the coordinates of that point whose mean-square displacement from a set of N bearing lines is minimal. Figure A-1 illustrates the geometry of the arrays, bearings, target, and coordinate origin. The directions of the x and y axes are specified by the unit vectors $\hat{i}$ and $\hat{j}$, respectively. The locations of the arrays relative to the origin are specified by the vectors $\underset{\sim}{r}_\alpha$ ($\alpha=1,2,\ldots,N$). The direction of the bearing line determined at the $\alpha$th array is specified by the unit vector $\hat{n}_\alpha$, which makes an angle $\phi_\alpha$ with the y axis.

The point to be determined is specified by the variable vector $\underset{\sim}{R}$, relative to the origin, and by the variable vector $\underset{\sim}{\chi}_\alpha$, relative to the $\alpha$th array. The displacement of the point from the $\alpha$th bearing line is given by the magnitude of the vector $\underset{\sim}{\varepsilon}_\alpha$. The distance from the $\alpha$th array to the foot of the vector $\underset{\sim}{\varepsilon}_\alpha$ is given by $d_\alpha$.

Since $\hat{n}_\alpha$ is a unit vector perpendicular to $\underset{\sim}{\varepsilon}_\alpha$, we have

$$\hat{n}_\alpha \cdot \hat{n}_\alpha = 1$$

$$\hat{n}_\alpha \cdot \underset{\sim}{\varepsilon}_\alpha = 0 \ . \qquad \text{(A-1)}$$

Since $\underset{\sim}{\chi}_\alpha$ can be expressed either as $\underset{\sim}{R} - \underset{\sim}{r}_\alpha$ or as $\underset{\sim}{\varepsilon}_\alpha + d_\alpha \hat{n}_\alpha$, we obtain

$$\underset{\sim}{\varepsilon}_\alpha = \underset{\sim}{R} - \underset{\sim}{r}_\alpha - d_\alpha \hat{n}_\alpha \ . \qquad \text{(A-2)}$$

Taking the scalar product of Eq. A-2 with the unit vector $\hat{n}_\alpha$, and

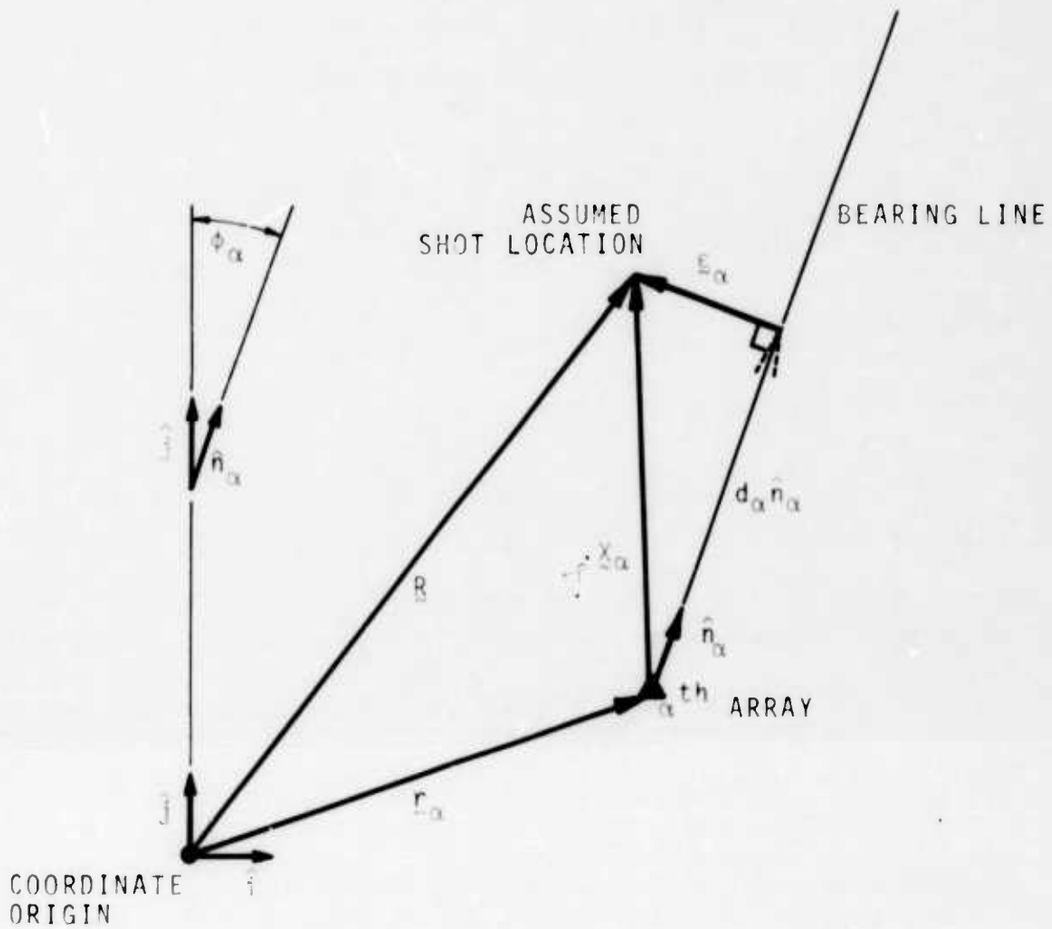


FIG.A-1 CONSTRUCTION FOR COMPUTING BEARING LINE DISPLACEMENT

applying Eq. A-1, we obtain an expression for $d_\alpha$:

$$d_\alpha = \hat{n}_\alpha \cdot (\underline{R} - \underline{r}_\alpha) \ . \qquad \text{(A-3)}$$

If we substitute this expression back into Eq. A-2, and then form the scalar product of the resulting equation with itself, we arrive at an expression for the squared magnitude of the displacement vector:

$$|\underline{\varepsilon}_\alpha|^2 = |\underline{R} - \underline{r}_\alpha|^2 - [\hat{n}_\alpha \cdot (\underline{R} - \underline{r}_\alpha)]^2 \ . \qquad \text{(A-4)}$$

The mean-square displacement of the assumed shot location from the N bearing lines is thus

$$\sigma^2 \equiv \frac{1}{N} \sum_1^N |\underline{\varepsilon}_\alpha|^2 = \langle |\underline{R} - \underline{r}|^2 \rangle - \langle [\hat{n} \cdot (\underline{R} - \underline{r})]^2 \rangle \ . \qquad \text{(A-5)}$$

(The angular brackets denote an average over the N arrays of the expression they enclose; for convenience, we delete all subscripts within the brackets.)

We now assume that the function $\sigma^2$ describes a concave surface as a function of the variable position of the vector $\underline{R}$. To find the minimum of this surface, we must equate the gradient of $\sigma^2$ to zero. This procedure determines two equations for the minimum point:

$$\langle (\underline{R} - \underline{r}) \cdot \hat{i} \rangle - \langle \hat{n} \cdot (\underline{R} - \underline{r}) \ \hat{n} \cdot \hat{i} \rangle = 0$$

$$\langle (\underline{R} - \underline{r}) \cdot \hat{j} \rangle - \langle \hat{n} \cdot (\underline{R} \cdot \underline{r}) \ \hat{n} \cdot \hat{j} \rangle = 0 \ . \qquad \text{(A-6)}$$

Expressing all vectors in terms of their cartesian components,

$$\hat{n}_\alpha = \hat{i}\,\sin\phi_\alpha + \hat{j}\,\cos\phi_\alpha$$

$$\hat{r}_\alpha = \hat{i}\,x_\alpha + \hat{j}\,y_\alpha$$

$$\underset{\sim}{R} = \hat{i}\,X + \hat{j}\,Y\ ,$$

we obtain the following pair of coupled linear equations:

$$\begin{pmatrix} \langle\cos^2\phi\rangle & -\langle\sin\phi\cos\phi\rangle \\ -\langle\sin\phi\cos\phi\rangle & \langle\sin^2\phi\rangle \end{pmatrix}\begin{pmatrix} X \\ Y \end{pmatrix} = \begin{pmatrix} \langle\cos\phi(x\cos\phi - y\sin\phi)\rangle \\ -\langle\sin\phi(x\cos\phi - y\sin\phi)\rangle \end{pmatrix}. \quad \text{(A-7)}$$

The condition for the existence of solutions of Eq. A-7 is that the determinant of the coefficient matrix does not vanish. Note that the coefficient matrix is entirely independent of the array locations; the array locations enter only in the inhomogeneous term. By means of simple algebraic manipulations, we can express the determinant in the form

$$\text{DET} = \frac{1}{4}\left[\left\langle(\cos 2\phi - \langle\cos 2\phi\rangle)^2\right\rangle + \left\langle(\sin 2\phi - \langle\sin 2\phi\rangle)^2\right\rangle\right]. \quad \text{(A-8)}$$

The determinant is the sum of the mean-square deviation of the cosine of twice the azimuth and the sine of twice the azimuth. Both of these terms can vanish only if all of the azimuths are equal. We conclude therefore that the MD prediction fails to exist only if all the bearing lines are parallel.

If the determinant does not vanish, the solution of Eq. A-7 for the coordinates of the MD prediction is

$$X = \frac{\langle \sin^2\phi \rangle \langle \cos\phi(x\cos\phi - y\sin\phi) \rangle - \langle \sin\phi\cos\phi \rangle \langle \sin\phi(x\cos\phi - y\sin\phi) \rangle}{\langle \sin^2\phi \rangle \langle \cos^2\phi \rangle - [\langle \sin\phi\cos\phi \rangle]^2}$$

$$Y = \frac{\langle \sin\phi\cos\phi \rangle \langle \cos\phi(x\cos\phi - y\sin\phi) \rangle - \langle \cos^2\phi \rangle \langle \sin\phi(x\cos\phi - y\sin\phi) \rangle}{\langle \sin^2\phi \rangle \langle \cos^2\phi \rangle - [\langle \sin\phi\cos\phi \rangle]^2} \quad . \tag{A-9}$$

Having obtained values of X and Y from this equation, we can find the rms deviation of the prediction from the bearing lines directly with Eqs. A-4 and A-5.

## APPENDIX B

### Generation of Synthetic Data for Testing of the Generalized Triangulation Algorithms

We assume a four-array configuration of azimuth-determining arrays as shown in Fig. B-1. Each individual array is the same as in Fig. 2. We postulate a group of 19 targets at locations shown on the map of Fig. B-2. The range and azimuth of each target relative to the center of the configuration (located at the central microphone of array 4) is given in Table B-I. The target field includes three closely spaced clusters along lines making different angles with the baseline of the configuration.

We postulate a series of one or more shots originating at each target at times given in Table B-I. Some targets are responsible for shots spaced less than thirty seconds apart. In addition, the shots emanating from each cluster of targets all occur in the same two- or three-second interval. The shot times are referred to the time of the first shot, which occurs at target 17. We number the shots from one to thirty-seven in order of their times of initiation.

From the geometry of the target and array locations, we calculate the true azimuth of each target relative to the center of each array (Table B-II). These are the azimuths which would be determined by a perfect azimuth determination algorithm.

The next step is polluting the azimuthal data to simulate the results of an imperfect azimuth determination algorithm (which is subject to azimuthal quantization and other errors). We altered each of the 148 shot azimuths (four azimuths for each of 37 shots) according to the following scheme:

(i) To each azimuth, add an increment of either -0.75°, -0.25°, +0.25°, or +0.75° with a one-fourth probability for each increment.

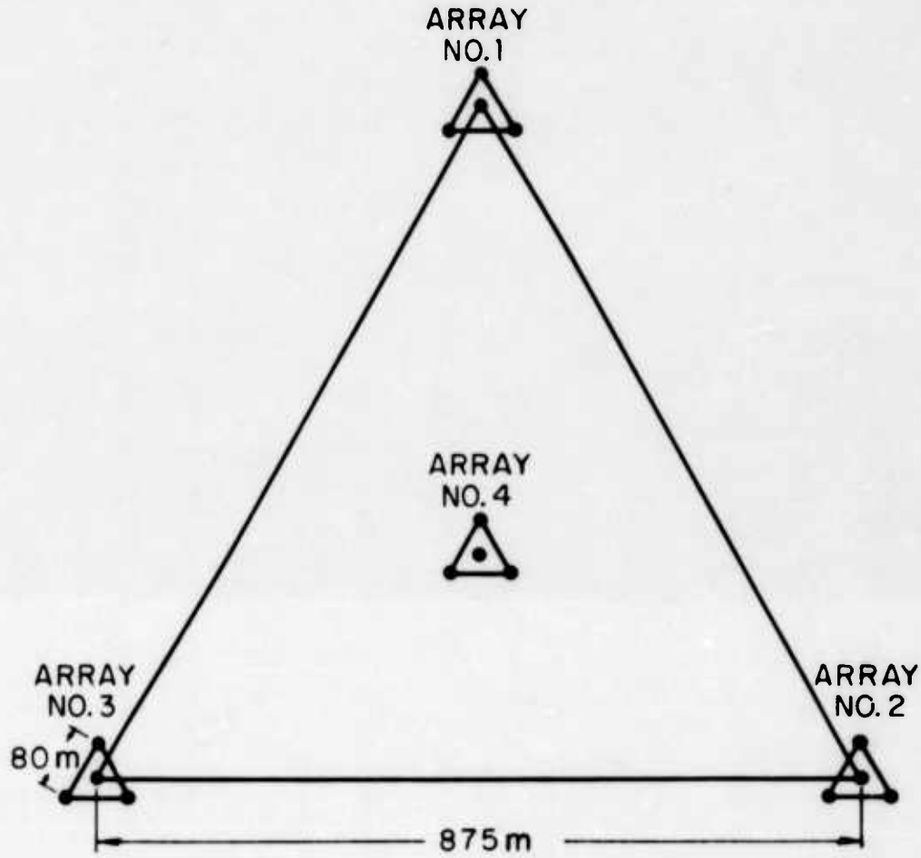


FIG.B-1 THE FOUR-ARRAY EQUILATERAL ARRAY CONFIGURATION

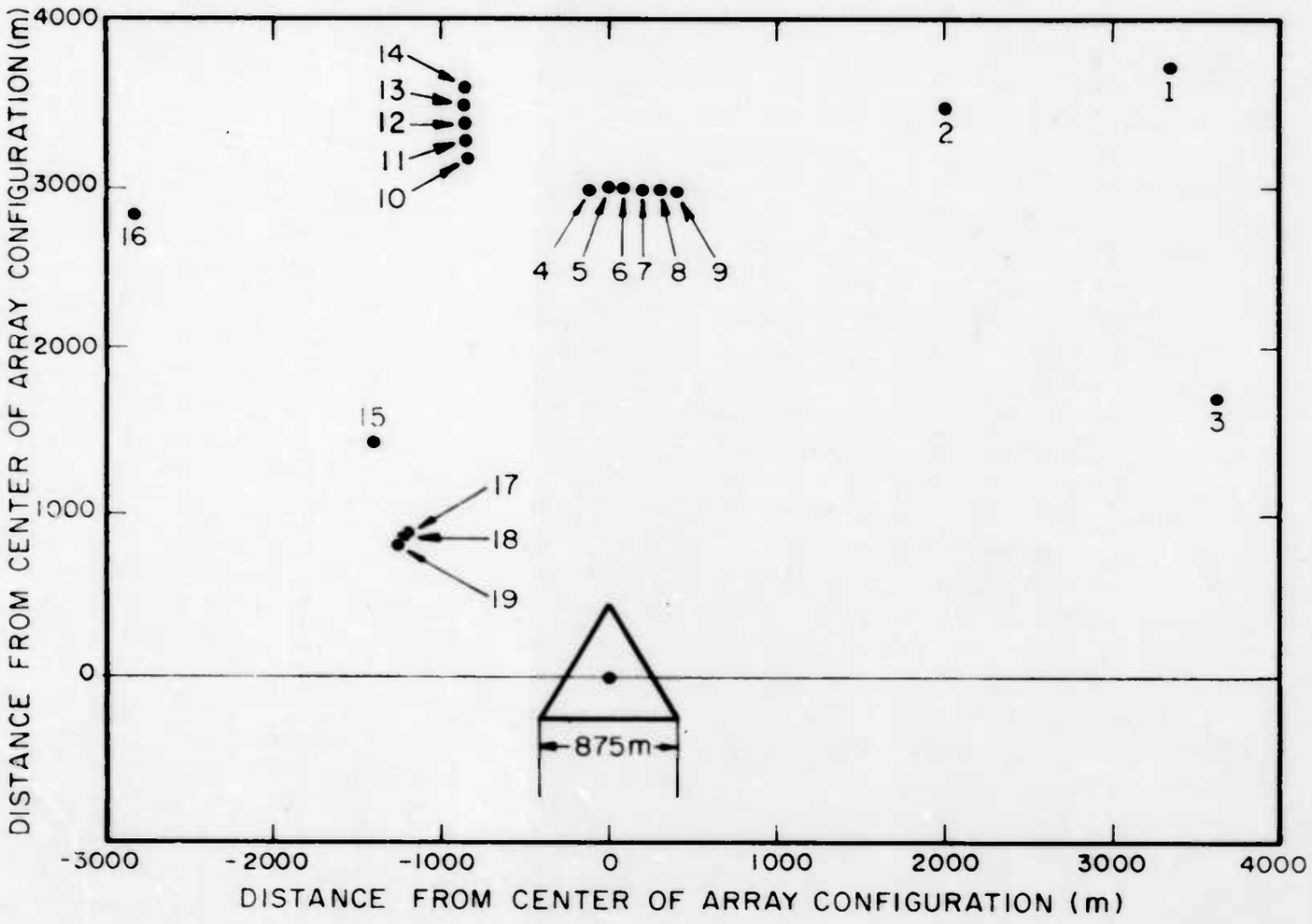


FIG.B-2 MAP OF ASSUMED TARGET LOCATIONS

TABLE B-I. Assumed target locations and shot times.

| Target | Range (km) | Azimuth (deg) | Shot Times (sec) |
|---|---|---|---|
| 1 | 5.0 | 42.2 | 30, 61, 88, 130, 180.25, 200 |
| 2 | 4 | 30 | 33, 62, 95, 120, 180.2, 205 |
| 3 | 4 | 65 | 34.5, 60, 110, 180, 210 |
| 4 | 3 | 358 | 63 |
| 5 | 3 | 0 | 62 |
| 6 | 3 | 1.8 | 62.5 |
| 7 | 3 | 4 | 62 |
| 8 | 3 | 5.8 | 63 |
| 9 | 3 | 8 | 64 |
| 10 | 3.306 | 345 | 71 |
| 11 | 3.403 | 345.4 | 71.5 |
| 12 | 3.500 | 345.9 | 72.5 |
| 13 | 3.597 | 346.2 | 72.75 |
| 14 | 3.694 | 346.7 | 74 |
| 15 | 2 | 314.8 | 110, 290, 360 |
| 16 | 4 | 315 | 100, 280, 340 |
| 17 | 1.5 | 306 | 0.0 |
| 18 | 1.5 | 304.8 | 0.3 |
| 19 | 1.5 | 304 | 0.45 |

TABLE B-II. True target azimuths at each array (to nearest 5').

| Target | Azimuth at Array 1 | Azimuth at Array 2 | Azimuth at Array 3 | Azimuth at Array 4 |
|---|---|---|---|---|
| 1 | 46° 20' | 36° 30' | 43° 55' | 42° 10' |
| 2 | 34° 05' | 22° 50' | 33° 15' | 30° 00' |
| 3 | 72° 00' | 58° 45' | 64° 30' | 65° 00' |
| 4 | 357° 35' | 350° 35' | 5° 55' | 358° 00' |
| 5 | 0° 00' | 352° 20' | 7° 40' | 0° 00' |
| 6 | 2° 15' | 354° 00' | 9° 25' | 1° 50' |
| 7 | 4° 45' | 355° 55' | 11° 15' | 4° 00' |
| 8 | 7° 05' | 357° 45' | 13° 00' | 5° 45' |
| 9 | 9° 35' | 359° 35' | 14° 50' | 8° 00' |
| 10 | 342° 25' | 339° 30' | 353° 10' | 345° 00' |
| 11 | 343° 00' | 340° 00' | 353° 25' | 345° 25' |
| 12 | 343° 35' | 340° 35' | 353° 30' | 345° 55' |
| 13 | 344° 10' | 341° 00' | 353° 40' | 346° 15' |
| 14 | 344° 30' | 341° 30' | 353° 50' | 346° 40' |
| 15 | 302° 30' | 311° 55' | 329° 30' | 314° 50' |
| 16 | 309° 15' | 313° 15' | 322° 05' | 315° 00' |
| 17 | 287° 05' | 304° 25' | 325° 30' | 306° 00' |
| 18 | 285° 50' | 303° 35' | 324° 30' | 304° 50' |
| 19 | 285° 05' | 303° 00' | 323° 30' | 304° 00' |

(ii) Round off each azimuth to the nearest half degree.

The distribution of errors resulting from this procedure is shown in Fig. B-3. The final shot azimuth sets for all 37 shots are presented in Table B-III. This is the data we use to test the generalized triangulation methods in Sec. 3.

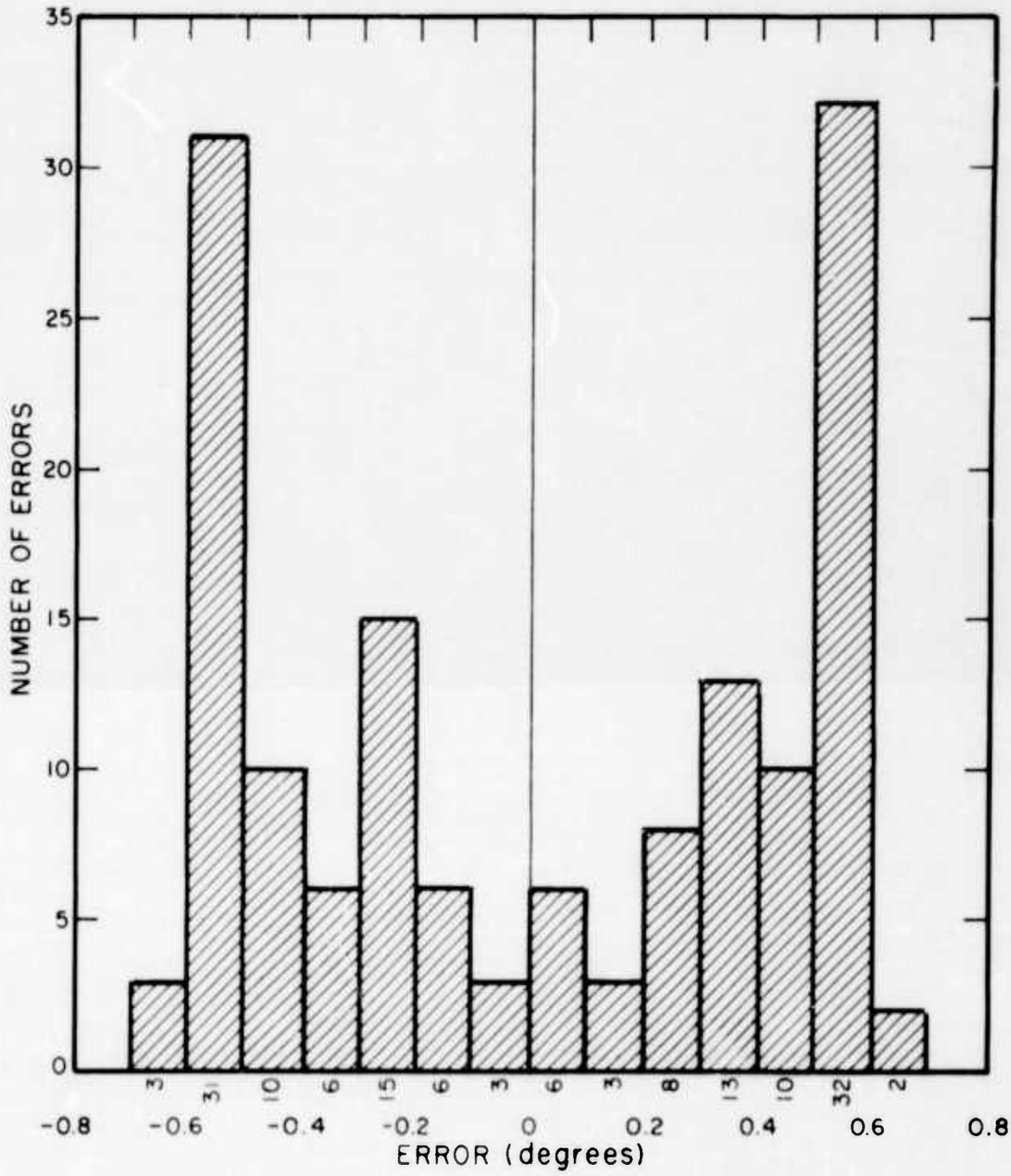


FIG.B-3 DISTRIBUTION OF SIMULATED SHOT AZIMUTH ERRORS

TABLE B-III. Shot azimuth sets with simulated errors.

| Shot | Target | Azimuth at Array 1 | Azimuth at Array 2 | Azimuth at Array 3 | Azimuth at Array 4 |
|---|---|---|---|---|---|
| 1 | 17 | 287.50° | 304.50° | 326.00° | 305.50° |
| 2 | 18 | 286.00° | 304.00° | 324.00° | 305.50° |
| 3 | 19 | 284.50° | 302.50° | 323.00° | 303.50° |
| 4 | 1 | 46.50° | 37.00° | 43.50° | 42.50° |
| 5 | 2 | 34.00° | 22.50° | 33.50° | 29.50° |
| 6 | 3 | 72.50° | 58.50° | 64.00° | 64.50° |
| 7 | 3 | 72.50° | 59.00° | 64.00° | 65.50° |
| 8 | 1 | 46.50° | 36.00° | 44.50° | 42.00° |
| 9 | 2 | 34.50° | 22.50° | 33.00° | 30.50° |
| 10 | 5 | .50° | 352.00° | 8.00° | .50° |
| 11 | 7 | 5.00° | 355.50° | 11.50° | 3.50° |
| 12 | 6 | 2.00° | 353.50° | 9.00° | 1.50° |
| 13 | 4 | 358.00° | 350.50° | 5.50° | 358.50° |
| 14 | 8 | 6.50° | 357.50° | 13.50° | 5.50° |
| 15 | 9 | 9.50° | 360.00° | 14.50° | 7.50° |
| 16 | 10 | 342.00° | 339.00° | 353.50° | 345.50° |
| 17 | 11 | 343.50° | 339.50° | 353.00° | 345.50° |
| 18 | 12 | 344.00° | 341.00° | 353.00° | 345.50° |
| 19 | 13 | 344.00° | 340.50° | 343.00° | 346.50° |
| 20 | 14 | 344.00° | 343.00° | 354.00° | 347.00° |
| 21 | 1 | 46.50° | 37.00° | 44.50° | 42.50° |
| 22 | 2 | 34.50° | 22.50° | 33.00° | 30.50° |
| 23 | 16 | 309.50° | 313.50° | 322.50° | 314.50° |
| 24 | 3 | 72.50° | 59.00° | 64.00° | 65.50° |
| 25 | 15 | 302.00° | 312.50° | 329.00° | 314.50° |
| 26 | 2 | 34.00° | 22.50° | 33.50° | 30.50° |
| 27 | 1 | 46.00° | 37.00° | 43.50° | 41.50° |
| 28 | 3 | 72.50° | 59.00° | 65.00° | 65.50° |
| 29 | 2 | 33.50° | 22.50° | 33.50° | 29.50° |
| 30 | 1 | 47.00° | 37.00° | 43.50° | 42.50° |
| 31 | 1 | 46.50° | 37.00° | 44.00° | 42.00° |
| 32 | 2 | 34.00° | 22.50° | 33.50° | 29.50° |
| 33 | 2 | 34.00° | 23.50° | 33.00° | 30.50° |
| 34 | 16 | 309.00° | 313.50° | 322.50° | 314.50° |
| 35 | 15 | 302.00° | 312.50° | 330.00° | 314.50° |
| 36 | 16 | 309.50° | 313.50° | 321.50° | 315.50° |
| 37 | 15 | 302.00° | 311.50° | 329.00° | 314.50° |

## REFERENCES


1. H.L. Fox, D.U. Noiseux, E.A. Starr, K.L. Chandiramani, and S.P. Robinson, "Signal Processing Techniques for Sound Ranging: Preliminary Studies," Tech. Rept. No. ECOM-0378-1, U.S. Army Electronics Command, Fort Monmouth, N.J. (Oct. 1967).

2. D.U. Noiseux and S.P. Robinson, "Signal Processing Techniques for Sound Ranging: Design - Part I," Tech. Rept. No. ECOM-0378-2, U.S. Army Electronics Command, Fort Monmouth, N.J. (Apr. 1968).

3. K.L. Chandiramani and H.L. Fox, "Signal Processing Techniques for Sound Ranging: Quantizing Delay Vectors," Tech. Rept. No. ECOM-0378-3, U.S. Army Electronics Command, Fort Monmouth, N.J. (June 1968).

UNCLASSIFIED

Security Classification

**DOCUMENT CONTROL DATA - R & D**

*(Security classification of title, body of abstract and indexing annotation must be entered when the overall report is classified)*

1. ORIGINATING ACTIVITY (Corporate author)

Bolt Beranek and Newman Inc.
50 Moulton Street
Cambridge, Massachusetts 02138

2a. REPORT SECURITY CLASSIFICATION

Unclassified

2b. GROUP

3. REPORT TITLE

SIGNAL PROCESSING TECHNIQUES FOR SOUND RANGING: FROM CORRELATION FUNCTIONS TO TARGET COORDINATES

4. DESCRIPTIVE NOTES (Type of report and, inclusive dates)

Interim Report: 1 January 1968 - 31 October 1968

5. AUTHOR(S) (First name, middle initial, last name)

6. REPORT DATE

December 1969

7a. TOTAL NO. OF PAGES

62

7b. NO. OF REFS

3

8a. CONTRACT OR GRANT NO.

DAAB07-67-C-0378

b. PROJECT NO.

1Z6 62704 D198 02

c.

d.

9a. ORIGINATOR'S REPORT NUMBER(S)

BBN Report No. 1746

9b. OTHER REPORT NO(S) (Any other numbers that may be assigned this report)

ECOM-0378-4

10. DISTRIBUTION STATEMENT

Each transmittal of this document outside the Department of Defense must have prior approval of CG, U.S. Army Electronics Command, Fort Monmouth, New Jersey. ATTN: AMSEL-HL-CT-P.

11. SUPPLEMENTARY NOTES

12. SPONSORING MILITARY ACTIVITY

U.S. Army Electronics Command
Fort Monmouth, New Jersey 07703
ATTN: AMSEL-HL-CT-P

13. ABSTRACT

This report considers the problem of predicting target coordinates, given a temporal and spatial distribution of shots from a multiplicity of targets. Our method is based on analyzing multifold polarity-coincidence correlations of acoustic signals received at a configuration of azimuth-determining arrays.

We review the process of generating multifold correlation functions, with emphasis on those properties which are of concern in azimuth determination. We describe an azimuth determination algorithm designed to make most effective use of the information contained in the correlation function.

Our discussion of generalized triangulation points out the weaknesses of traditional methods, and outlines a probabilistic approach to triangulation that would yield an optimal prediction for a given set of azimuths. Because this probabilistic approach would be extremely demanding in computational requirements, we present an alternative method based on similar concepts but yielding a closed-form solution. This new method of generalized triangulation is tested with synthetic data, and found consistently more accurate than the traditional method.

DD FORM 1 NOV 65 1473 (PAGE 1)

S/N 0101-807-6811

UNCLASSIFIED

Security Classification

A-3140

| 14 KEY WORDS | LINK A | | LINK B | | LINK C | |
|---|---|---|---|---|---|---|
| | ROLE | WT | ROLE | WT | ROLE | WT |
| Sound ranging | | | | | | |
| Data reduction techniques | | | | | | |
| Microphone arrays | | | | | | |
| Polarity coincidence correlation | | | | | | |
| Azimuth determination | | | | | | |
| Generalized triangulation | | | | | | |